



Limited-damage 3D-printed interlocking connection for timber volumetric structures: Experimental validation and computational modelling

Zhengyao Li^a, Konstantinos Daniel Tsavdaridis^{b,*}

^a School of Civil Engineering, Faculty of Engineering and Physical Sciences, University of Leeds, Woodhouse Lane, LS2 9JT, Leeds, UK

^b Department of Engineering, School of Science and Technology, City, University of London, Northampton Square, EC1V 0HB, London, UK

A B S T R A C T

Cross laminated timber volumetric construction (CLTVC) is an innovative construction technology that combines the sustainability of timber and the efficiency of modular construction, as opposed to conventional construction. However, the connection installing methods of CLTVC, such as fastening, are laborious with limited accessibility for connection installations, thus hindering the application of CLTVC in mid- and high-rise structures. Therefore, a new way of connecting CLT modules by sliding and stacking is explored herein with a newly proposed damage-control interlocking connection system, aiming to provide a more efficient assembly solution to CLTVC that does not require onsite screwing. Quasi-static monotonic and cyclic test, and numerical analyses were conducted to assess the mechanical performance of the proposed connections, which possessed adequate translational stiffness and strength of the proposed connections. The connections' ability to control deformation, while damage is moved away from timber and the embedded fasteners, was also well demonstrated in the test, as both screws and timber remained mostly intact after testing. This novel connection design showcases a new concept of modules' assembly in volumetric construction with higher efficiency and flexibility; meanwhile demonstrates the potential in reducing the permanent damage to structural materials during service life and enabling reuse.

1. Introduction (recent studies, new interlocking connections and their limitations)

1.1. Multi-storey timber volumetric construction

Volumetric construction is an emerging modern method of construction (MMC) that has the highest degree of prefabrication (~95%) [1] with the main structure and other building accessories such as cladding, internal finishes and MEP services all being manufactured and assembled into flat modules in factories (offsite manufacturing - OSM) before being transported to sites for the final assembly. With the advent of automation and the future factories (the fourth industrial revolution), better quality and higher precision of assembly work compared to the on-site manual operation can be ensured in volumetric construction. Being able to combine the sustainability of timber materials and the efficiency of the OSM, volumetric timber construction is considered as one of the direct solutions to the growing demand in affordable urban accommodation as well as the high carbon footprint problem own to the construction industry [2]. Yet, this construction technology is limited to mid- and low-rise structures [2], and the current trend of building tall volumetric timber structures imposes new challenges on the wind and seismic resistances of such structural systems, requiring further investigations on varied aspects of VTC; for example updates on design strategy in standards, high-performing connection systems and assembly tools, as well as the development of more accurate numerical modelling methods [3] for the confident delivery of secured high-rise volumetric timber structures.

* Corresponding author.

E-mail address: Konstantinos.tsavdaridis@city.ac.uk (K.D. Tsavdaridis).

1.2. Conventional timber connection systems for multi-story VTC

Among all the currently available forms of timber volumetric structures, the Cross Laminated Timber (CLT) volumetric structure that employs load-bearing CLT panels, has somewhat better potential over others (e.g., Framed Volumetric Structures and Structural Insulated Panels, SIPs) to be used for tall buildings due to the high stiffness of CLT. However, suitable connections for this structural system still lack sufficient investigation, as it is a relatively new construction technology. In volumetric construction, the connections between modular units, also known as inter-module connections, are critical to both the project efficiency and the overall structural performance of the buildings, as they link prefabricated modular units together on-site to form the entire structure and are designed to transfer horizontal and uplift forces from the wind and seismic actions. Previous quasi-static tests on CLT panelised systems [4,5] and shake table tests on full-scale low-rise CLT buildings [6,7] indicated that structures made of CLT panels generally demonstrated high strength and stiffness with most of the deformation and energy dissipation being processed in connections and friction between timber panels. Therefore, the proposal of high-performing connections is crucial to the realisation of high-rise volumetric CLT structures with improved wind and seismic performances.

Angle brackets and hold-downs (Fig. 1) are the commonly used shear and tensile connections in timber construction, which are originally designed for post-and-beam timber structures, so they are not fully applicable in CLTV. Some well-known disadvantages of these connection systems in both construction and structure aspects currently limit their application in high-rise CLT volumetric structures. To name a few:

1.2.1. Incompatibility with CLTV and low construction efficiency

The limited accessibility is a widely recognised challenge in volumetric construction. The installation of conventional timber

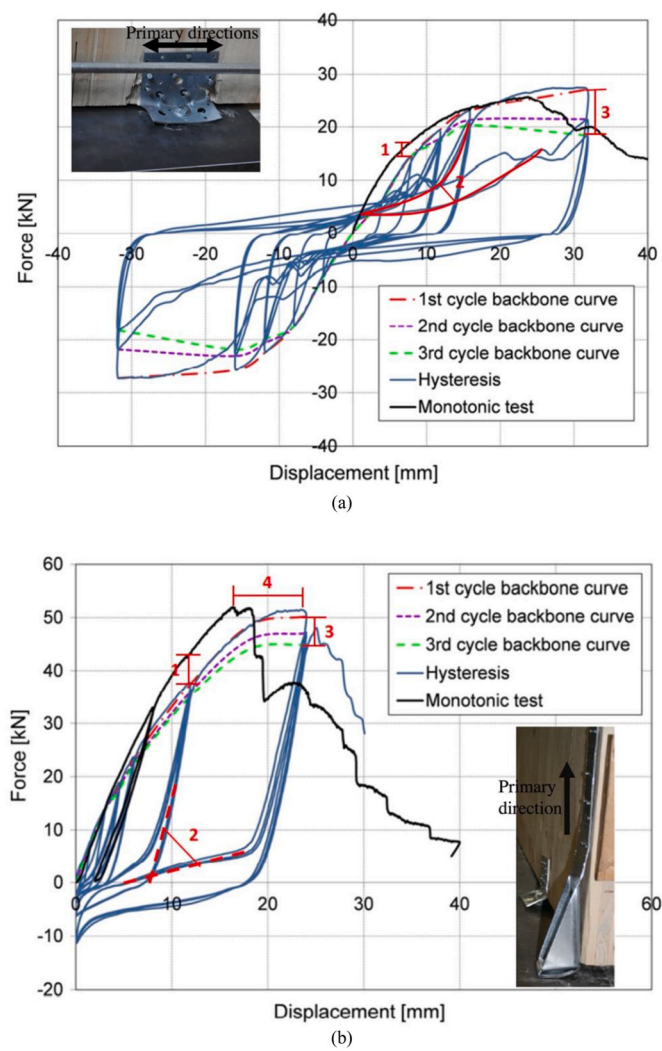


Fig. 1. Typical CLT connections (a) angle bracket and (b) hold-down and their representative monotonic and cyclic responses and failure modes on the primary working directions [8].

connections requires external access, while accessibility for inter-module connections has long been a key challenge in volumetric construction [9], especially when CLT modules become enclosed as panelised structures, which makes the inter-module connections in CLTVC entirely inaccessible (Fig. 2). Consequently, in some CLT volumetric structures [2,10], the inter-module connections are absent and the lateral resistance of the structure is provided by the friction between modules or the additional structural reinforcing systems, such as steel frames and concrete cores. This method is commonly adopted in low-rise CLTVC and the inaccessibility of inter-module connections is treated as one of the main obstacles to achieving tall CLT volumetric structures with sufficient lateral stiffness, considering the importance of inter-module connections in defining the integrity and stability of volumetric structures.

1.2.2. Insufficient mechanical properties

According to the published experimental studies [8,12], both angle brackets and hold-downs are characterised by high stiffness and strength but insufficient ductility (belonging to L or M ductility class as prescribed in EC8 [13]) in their primary directions (Fig. 1(a)&(b)). In the cyclic tests on conventional connections, several hallmarks can be observed (Fig. 1): (1) the reduced maximum strength at each step than that in monotonic test at the same displacement amplitude, (2) the stiffness degradation happens at load reversals, (3) the strength degradation occurs during the repeated cycles at the same displacement, (4) the delayed attainment of maximum strength in cyclic test compared to monotonic test.

The above-mentioned features are attributed to the cavities around fasteners formed by the crushing of timber and the deformation of fasteners during loading, which damage the capacity of surrounding timber and are highly unfavourable to the seismic design of high-rise structures, as they make the connection cyclic behaviours unpredictable and reduce the structure's capacity of energy dissipation during seismic events [14].

In addition, as the connection is the governing factor of the timber structures' ductility, the common concept of designing ductile timber structures is achieved by increasing the number of connections while using small-diameter fasteners. Large number of conventional connections with slender fasteners are therefore commonly adopted in large timber structures to achieve desired structural capacity (Fig. 3), which leads to time-consuming on-site fastening work that negatively impacts the project progress. This also limits the maximum reclamation and the reuse of timber components at the end-of-life of buildings, as the removal of nails and screws is labour-intensive and can damage the structural material [15]. Another concern of using small-diameter fasteners is the high stress they introduce on timber after experiencing significant deformation at the later stage of loading, which can pinch through the fibres before the capacity in timber is fully developed (Fig. 4(a)), causing sudden drop in connection strength and great residual displacement even after the removal of the external loading. This can be considered as brittle failure and cause irreversible damage to the structural elements, which results in difficulties in structural maintenance and should be avoided in connection design.

1.2.3. Insufficient accuracy in analytical models for connection capacity calculation

Comparative studies between analytical models and experiment results were conducted in previous research [8,12], which indicated that the existing analytical models for timber connections provide conservative predictions on connection strength but seems to

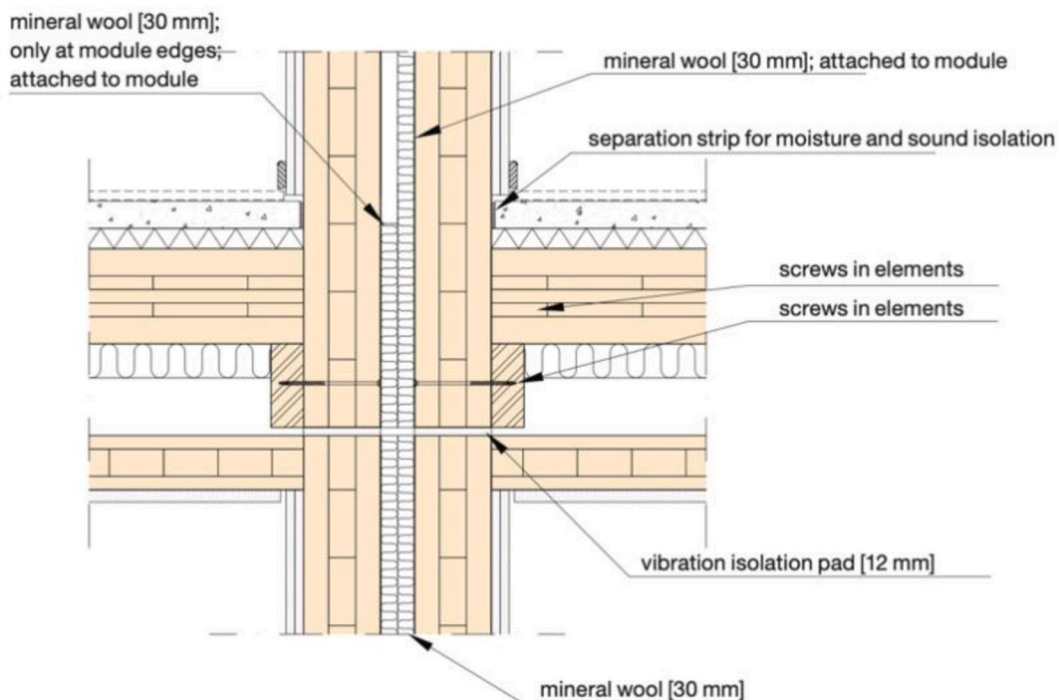


Fig. 2. Illustration of inaccessible inter-module connection between CLT modules [11].



Fig. 3. Numerous angle brackets used on a single CLT shear wall to achieve sufficient capacity and ductility.

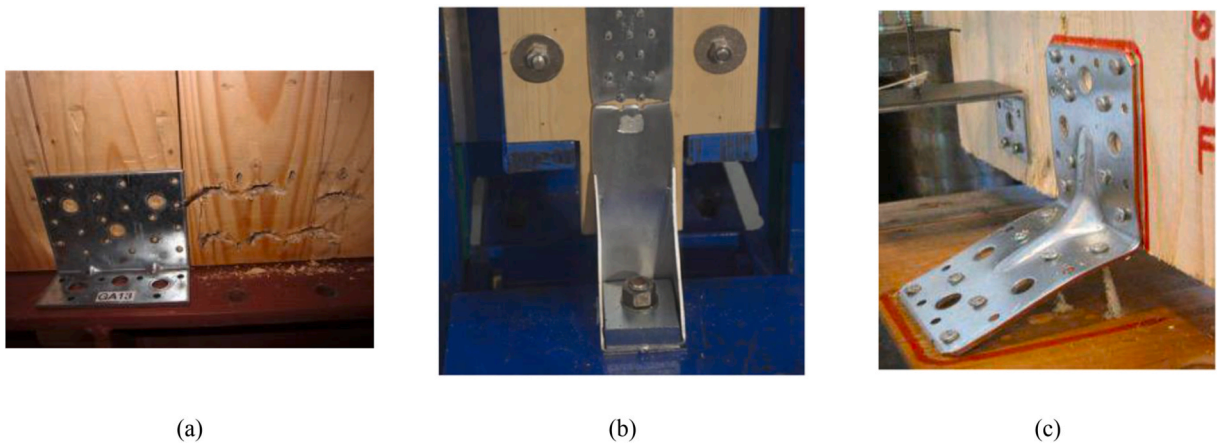
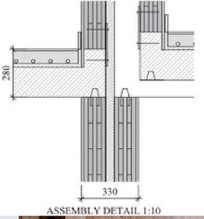
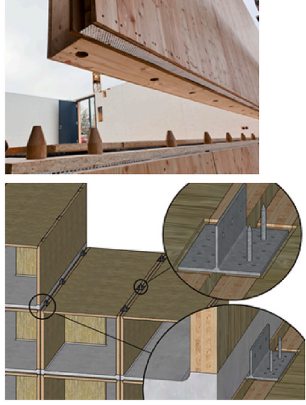
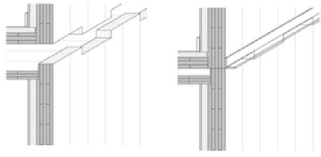
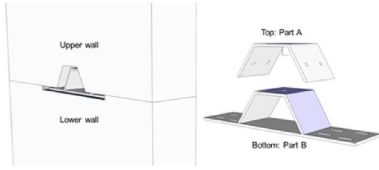


Fig. 4. Possible deformation modes in timber connections: (a) localised deformation on fasteners with timber fibres being cut through [8] (b) brittle failure on metal flange (c) combination of bending of plate, splitting of timber and withdrawal of screws [20].

significantly overestimate the stiffness (up to 9 times higher according to the study of Gavric and Fragiaco [8]). One potential source of errors in the analytical models can be the assumption of brittle elements (timber) and ductile elements (fasteners and steel plate) working independently, with the embedding strength of timber and the yield moment of fastener being considered separately in calculations. This is because typical timber connections are composite structures, in which deformation happens simultaneously in ductile and brittle elements when loaded (Fig. 4(b)&(c)). Hence, considering the strength of different components independently and ignoring the composite effect when estimating the overall capacity of the connection could lead to significant differences between the actual strength and the calculated value. The much bigger actual strength of the embedded fasteners than the design value that was estimated with Johansen's theory in EC5 [16], and the overestimations of the stiffness and strength of the brittle elements due to the much greater scattering of timber material properties than steel material [17], can also lead to inaccurate estimations in connection design, which may cause non-ductile failure modes in connections (e.g., splitting of timber) [8,12].

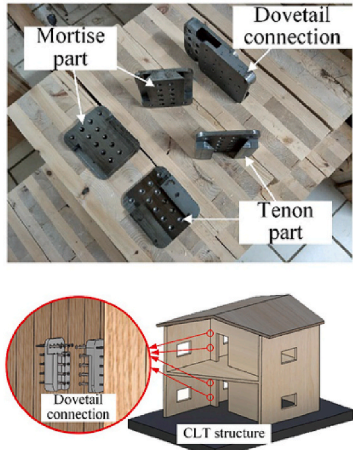
The afore-mentioned factors also affect the overstrength method that widely adopted in the research and practice of timber structures, which is developed by Jorissen and Fragiaco (Eq. (1)) [18] based on capacity-based design method to ensure the full activation of all ductile elements before the non-ductile area enters the plastic stage [19]. In this method, an overstrength factor γ_{Rd} accounting for all possible factors that may lead to unexpected high strength in ductile elements ($R_{d,ductile}$) (underestimated material strength, potential strain hardening and contribution of steel plate at large deformations) is introduced in the design strength of brittle elements ($R_{d,brittle}$) (Eq. (1)).

Table 1
List of innovative interlocking connection systems for CLT structures.

Name	Connection Fig.s	Comments	Ref
<p>Novel connections for CLT volumetric structures Heidelberg Student Accommodation</p>		<p>A bespoke interlocking inter-module connection for the easy installation of CLT flat modules.</p>	[2]
<p>Jakarta Hotel</p>		<p>A steel T-shaped angle plate with pins for the accurate alignment and translational constraints of modules</p>	[23]
<p>Moxy Modular Hotels (Marriott)</p>		<p>A specially designed notched CLT panel used as the side wall of modules and the inter-module connection for the easy on-site modules assembly.</p>	[2]
<p>A novel inter-module horizontal connection proposed by the University of British Columbia</p>		<p>A replaceable inter-module connection to achieve good energy dissipation and limit plastic deformation in timber.</p>	[24]
<p>Interlocking connections for CLT panelised structures LOCK Connection from Rothoblaas Ltd.</p>		<p>A concealed, interlocking wall-to-floor connection for CLT structures. The Lock Connection is attached on the surfaces or edges of wall and floor CLT panels, so the floor panels can be slid into the right positions to connect with wall panels, eliminating on-site fastening work.</p>	[25]

(continued on next page)

Table 1 (continued)

Name	Connection Fig.s	Comments	Ref
Metal dovetail connection		An interlocking connection inspired by traditional mortise and tenon joints and designed for the quick assembly of CLT panels.	[26]

$$\gamma_{Rd} R_{d,ductile} \leq R_{d,brittle} \tag{1}$$

This factor is defined as the ratio of the 95th-percentile strength distribution to the analytical design strength capacity of the connection [18]. The inaccurate estimations of analytical models can lead to the adoption of inappropriate overstrength factors, which may further result in the overdesign of structural material or the unfavourable connection behaviours.

1.3. Innovative connection systems

To address the limited accessibility of inter-module connections in volumetric construction, a new way of assembling flat modules using interlocking techniques was explored in previous research [21,22]. These conceptual studies demonstrate the potential of

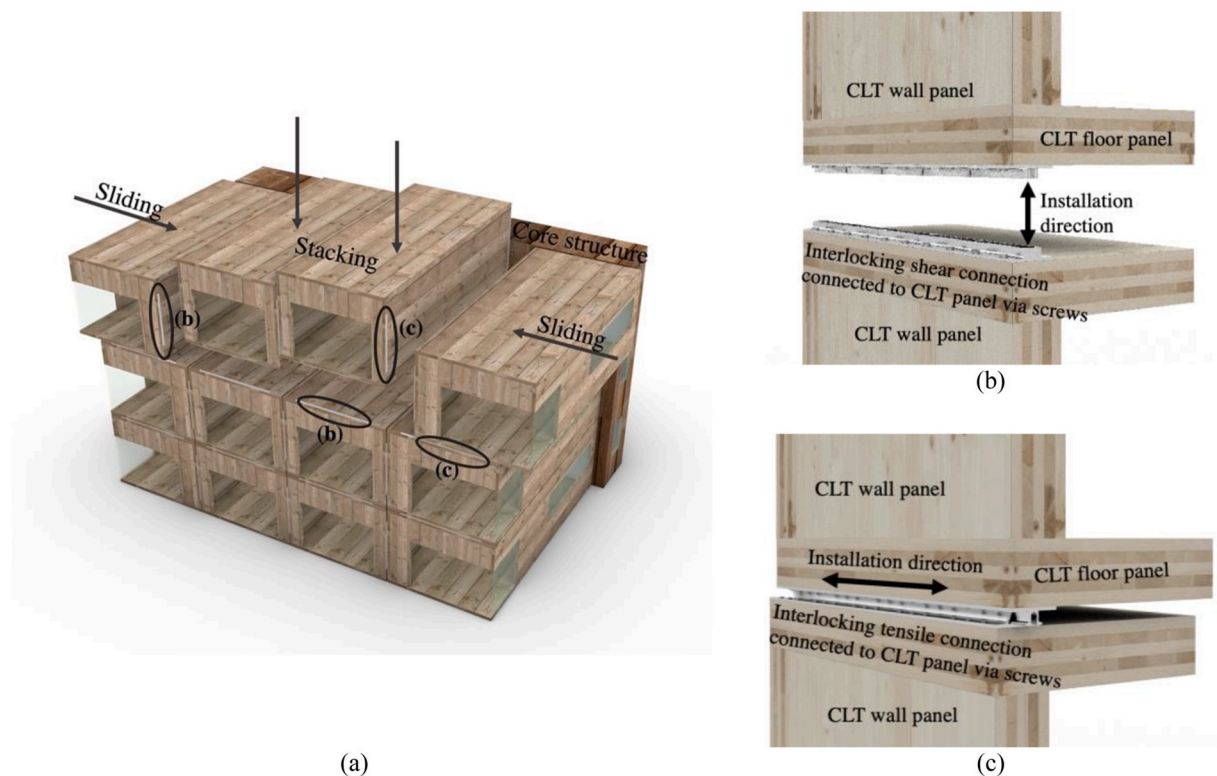
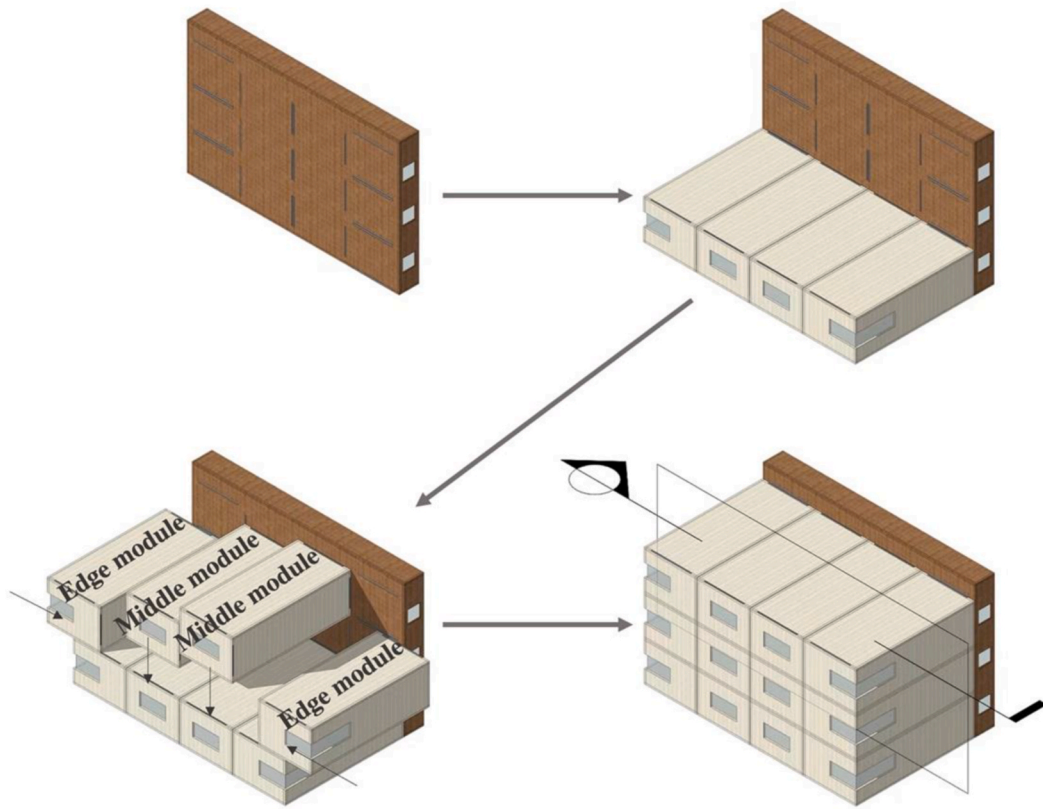
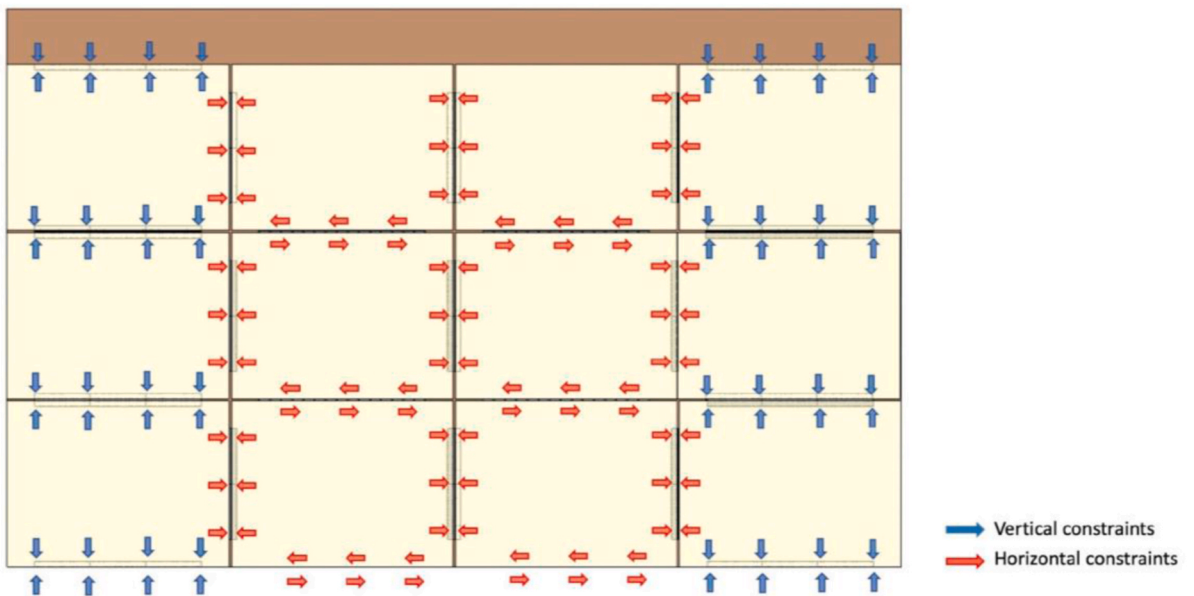


Fig. 5. Overview of the novel interlocking connection system for VTC: (a) Locations of connections in a CLT volumetric structure and the assembly of CLT modules with the pre-installed connections (b) the stacking of interlocking shear connection (c) the sliding of interlocking tensile connection.



(a)



(b)

(caption on next page)

Fig. 6. The illustrations of the working mechanism of the interlocking connection system (a) the modules assembly process with the interlocking connection system (b) the sectional elevation of the structure showing the overall constraints provided by the integrated interlocking connection system.

interlocking technique in achieving replaceability, adaptability and dismantlability in volumetric structures. This technique was also employed in the design of some recently proposed connection prototypes for CLT volumetric structures, as summarised in Table 1. These new connections eliminate the onsite manual operation in CLTVC needed for screwing, so that the access to inter-module connections is not required, and better construction efficiency and accuracy can be achieved. Similar interlocking design can also be observed in some new connections proposed for CLT panelised structure (Table .1). These recent developments enrich the importance of interlocking technique in CLT connection systems for efficient construction and upgraded structural performance. However, the listed interlocking connections for CLTVC are all bespoke connection solutions proposed for specific projects, while a universal interlocking connection solution for CLTVC has not yet been proposed. And these bespoke connections all require special modifications on CLT panels for the fitting of connections, which limit their applications in other CLT volumetric structures.

In some novel connections [27–31] designed for CLT panelised structures, another commonly adopted design strategy is to introduce an individual ‘weak component’ in the connections to control the plastic deformation. By applying capacity-based design to strengthen timber and fasteners, this design strategy can efficiently isolate timber from deformation and localise the deformation within the additional metal connectors. In this way, much improved strength and ductility can be achieved in connections with reduced risks of brittle failure, considering the limited ability of timber to deform plastically. A similar approach is also widely adopted in the recent proposals of dissipator [32–35] for CLT structures.

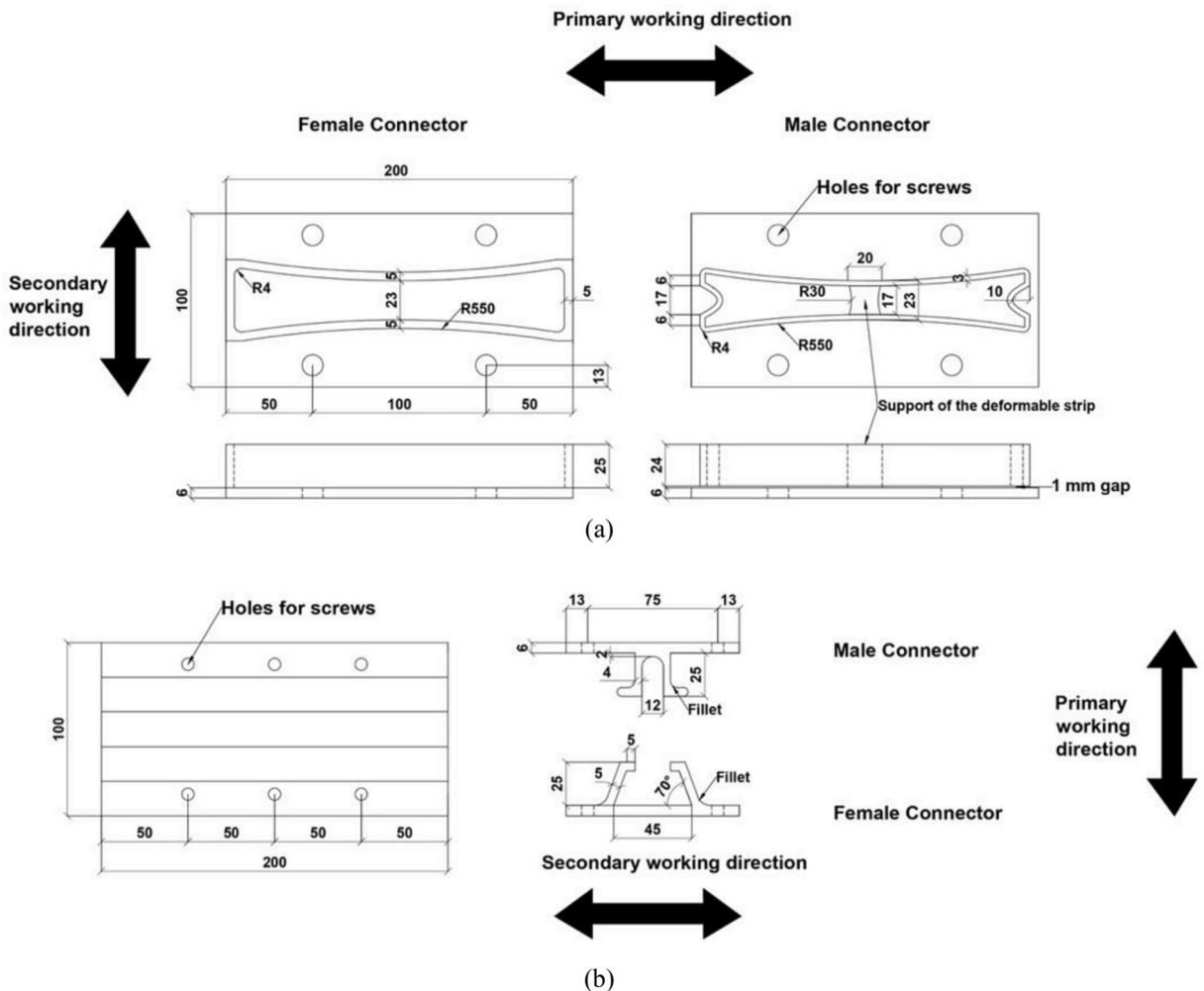
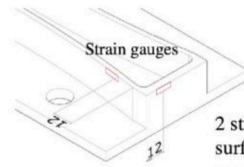
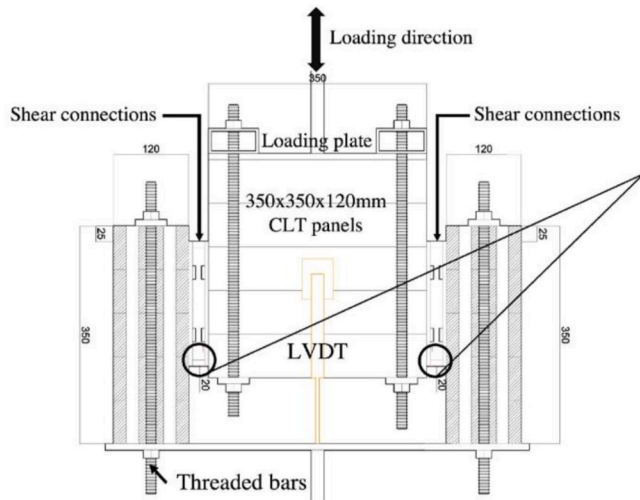


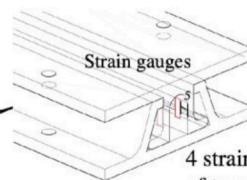
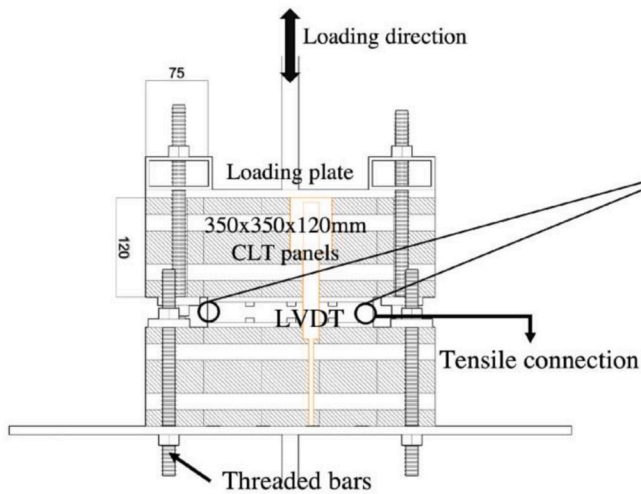
Fig. 7. Schematic the basic units of interlocking connection (in mm): (a) shear connection (b) tensile connection.



2 strain gauges at the external surface of each shear female connector



(a)



4 strain gauges at the inside of tensile male connector at both ends



(b)



(c)



(d)

(caption on next page)

Fig. 8. Experimental set-ups for (a)&(c) shear connection and (b)&(d) tensile connection.

2. Novel interlocking connection system for CLT modules

2.1. Concept of the interlocking connection

In order to achieve enhanced structural performance in multi-storey CLT volumetric structures and simplify the module assembly process, a novel interlocking inter-module connection system is herein proposed. This connection system consists of both vertical and horizontal connections that can be pre-installed onto CLT modules in the factory (off-site) (Fig. 5(a)). It is suitable for most of the module specifications, as it requires no further modification on panels for the fitting of connection, which can greatly simplify and standardise the structural design process and become available to the entire market. Owing to its interlocking feature, the modules can be accurately assembled on-site by sliding and stacking without the need for additional tooling and special operations (Fig. 5(b)&(c)), so the on-site assembly of modules will no longer be constrained by the access of inter-module connections and the erection process of CLT volumetric structures can be significantly sped up.

Due to the interlocking technique, both shear and tensile connections of this new system are not fully rigid in their installation directions and are designed to transmit shear or tensile forces only (Fig. 6(b)). After assembly, the movement of connectors can be locked by simple end-locking systems (i.e. extended plates with holes welded on the ends of the connectors, through which fasteners can fix two connectors). The full integration of constraints on the structure in both horizontal and vertical directions is achieved by the strategic placement of modules. In the CLTVC with interlocking connections as illustrated in Fig. 6, the core structure used as lift shaft or staircase is first constructed with preinstalled connections. Following the arrangement of the connections on the core structure, the flat modules with pre-installed connections can simply slide over or be stacked into the correct positions (Fig. 6(a)). The illustrated strategic assembly can form a continuous vertical reinforcement along the edge modules and a horizontal reinforcement along the middle modules (Fig. 6(b)), resisting the uplifting and inter-storey drift caused by external forces. The continuous reinforcement provided by this connection strip design can also minimise load concentration on CLT panels as well as provide a certain amount of bending resistance, though bending moment is often neglected in CLT building design due to the high in-plane stiffness of CLT panels. This kind of edge-supporting connection system, as proved by the previous numerical analysis on similar interlocking connection [21], can help achieve enhanced integrity in volumetric structures. When damage happens in the connection units of one of the modules, the entire structures can remain stable with little movement and require no need for immediate replacement, because alternative load path can form along the edges of the remained modules, reassuring that the performance requirements is still satisfied. In addition, located at the exterior surface of modules, the interlocking connections are invisible from the interior of flats and can be protected from the external environment by the façade after the completion of the project.

2.2. Description of the unit elements of the interlocking connectors

Both tensile and shear connections have female connectors and male connectors, and each of them consists of repetitive unit patterns as demonstrated in Fig. 7. Their width is being determined according to the dimensions of conventional plate connections. The thickness of the bottom plate in all connectors was chosen based on the common practice of having steel plate thickness as $0.5d$ in double shear timber joints, to achieve adequate strength and avoid local deformation in the vicinity of screws [36]. The female connectors of both connections are groove-like devices, which are designed for accommodating the male connectors. The male connector in shear connection is formed by a cantilevering thin-walled curved steel band connected to a bottom steel plate via a cubic support at the middle, which is designed to deform during movement. In the unit element of the tensile male connector, two symmetric L-shaped steel components are connected to the steel plate with a 12 mm gap in between for their free inward movement when sliding along the sloping walls of the female connector. The width of the gap was chosen corresponding to the maximum horizontal movement of the L-shaped components within the female connector before reaching the top part. Both male connectors are designed to act as the

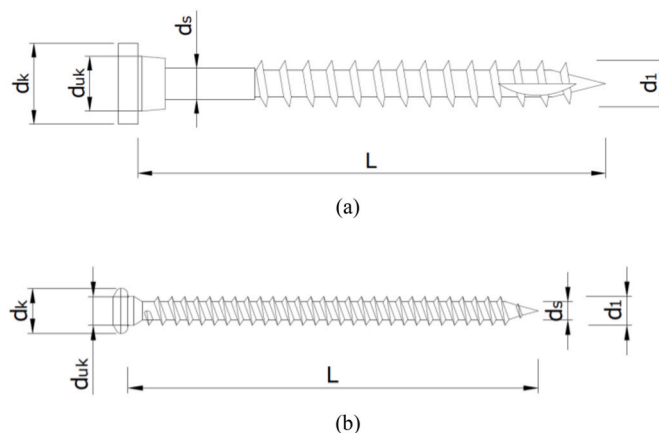


Fig. 9. Dimensions of screws: (a) HBSP12120 (b) LBS7100.

damage control devices of the system and to yield first to isolate most of the deformation (without damaging other integral parts of the connections) before reaching the target displacement, so the female connectors, the timber and the fasteners can remain mostly intact (undeformed). In this way, the male connectors become the critical components that determine the strength and ductility in the interlocking connection, which ensure more predictable behaviours due to the less scattering properties of steel than timber. This can also contribute to a more reliable (finite element) simulation with only basic material properties such as compressive strength and tensile strength of timber and steel being used. Moreover, as the ductility in this interlocking connection is designed to be achieved in the steel connectors instead of the fasteners, large diameter screws ($\varnothing 7 \text{ mm}$ - $\varnothing 14 \text{ mm}$) are used in this connection system, which as suggested in the literature [8,14], can improve load distribution and help to reduce the risk of in-service damage or brittle failure in timber. It is worth noting that in case of changing the damaged parts (units) of the connections, only the panels with the male connectors need removing.

3. Experimental testing

To assess the realistic performance of the proposed connection design and to develop reliable numerical models that can accurately simulate the connection performance, monotonic and cyclic tests were conducted on full-scale shear and tensile connection unit elements.

3.1. Test configuration and testing material preparation

Experimental set-ups for shear and tensile connections are shown in Fig. 8. To achieve symmetric test set-up for avoiding a moment being applied to the testing apparatus that may cause instability, two shear connections were tested together with three panels, while each tensile connection was tested individually. Overall, 3 monotonic tests (3 specimens) were conducted on the tensile connection and 1 (2 specimens) on the shear connection under the rate of 0.05 mm/s, and 2 cyclic tests (2 specimens) were performed on tensile connection and 1 (2 specimens) on shear connection under the speed of 0.02 mm/s. In the quasi-static (cyclic) test, the loading protocol as prescribed in EN12512 [37] was adopted, with the estimated yield point V_{est} of 4 mm for tensile connections and 2 mm for shear connections according to the preliminary FE simulations. 4 strain gauges were attached to the specimens in each test with the locations of which being decided considering the preliminary numerical simulations and the accessibility of the assembled connections (Fig. 8).

All connection specimens were connected to 5-ply GL24h 350mmx350mmx120mm CLT panels with density varied between 435 and 470 kg/m³ provided by Stora Enso using LBS7100 for the tensile connections and HBSP12120 for the shear connections. The locations of specimens on timber panels were all marked before the testing to measure the relative movement between timber and the steel connector. After being screwed to CLT panels, connection specimens were assembled by stacking (shear connection) or sliding (tensile connection) to form the experimental set-up and were tested without additional reinforcement. Mechanical and geometric properties of panels and screws are listed in Table 2 and Table 3. All CLT panels were conditioned in a controlled environment of 20 °C with 65% humidity for the week before testing in accordance with EN 1380 [38], and all achieved the moisture content of 10%–10.8%, which were within the required range in the standard (10%–14%).

The proposed novel connection specimens were 3D printed. Additive manufacturing was selected for its limitless fabrication capabilities, considering the new complex geometry with inclined and curved surfaces and the cantilevered steel band (Fig. 10(b)&(d)) of the proposed optimised connection designs. For the size of the proposed connections (Fig. 7), a metallic alloy composed of 60% 420 Stainless Steel as base material and 40% Bronze for additional strength and resistance was chosen in the printing with layer thickness of 100 μm using Binder Jetting in Sculpteo [40]. The connection specimens were printed along the length of connection. This printing direction was chosen to achieve the most stable printing process and minimise the potential deformations in the cantilevering parts. Surface polishing was not an option for this size of specimens from the manufacturer, thus the 3D printed connections were all finished with granular surface (Fig. 10). To eliminate the risk of unpredictable behaviour due to the variation of friction during the movement of male connections within the female connections, the contact surfaces were polished to obtain smooth surfaces before testing. Despite the high manufacturing accuracy of 3D printing, 1 mm tolerance was introduced in the printing of all connection specimens, to avoid the potential fitting issues caused by the dimensional distortion, considering the cantilevered feature and the scale of printing in this project. In the testing of tensile connections, the remaining gap after assembly was eliminated using the built-in function in the loading machine, while it is not achievable in the cyclic testing on the shear connections due to the reserve loading. Therefore, small amount of sliding with no reaction force can be observed at the beginning of each loading step in the cycling testing on the shear connections (see Fig. 21).

Table 2
Material properties for CLT panels (spruce) [39].

Elastic modulus (MPa)			Poisson's ratio			Shear modulus (MPa)		
E_{11}	E_{22}	E_{33}	ν_{12}	ν_{13}	ν_{23}	G_{12}	G_{13}	G_{23}
11000	370	370	0.48	0.48	0.22	690	690	50
Parallel-to-grain (MPa)			Perpendicular-to-grain (MPa)			Shear strength (MPa)		
f_{c11}	f_{t11}		f_{c22}	f_{t22}		f_v	$f_{v,roll}$	
36	24		4.3	0.7		6.9	0.5	

Table 3
Dimensions of screws used in experiment (in mm).

	L	d ₁	d _s	d _k	d _{uk}
HBSP12120	120	12	8	20.75	14
LBS7100	100	7	4.4	11	7

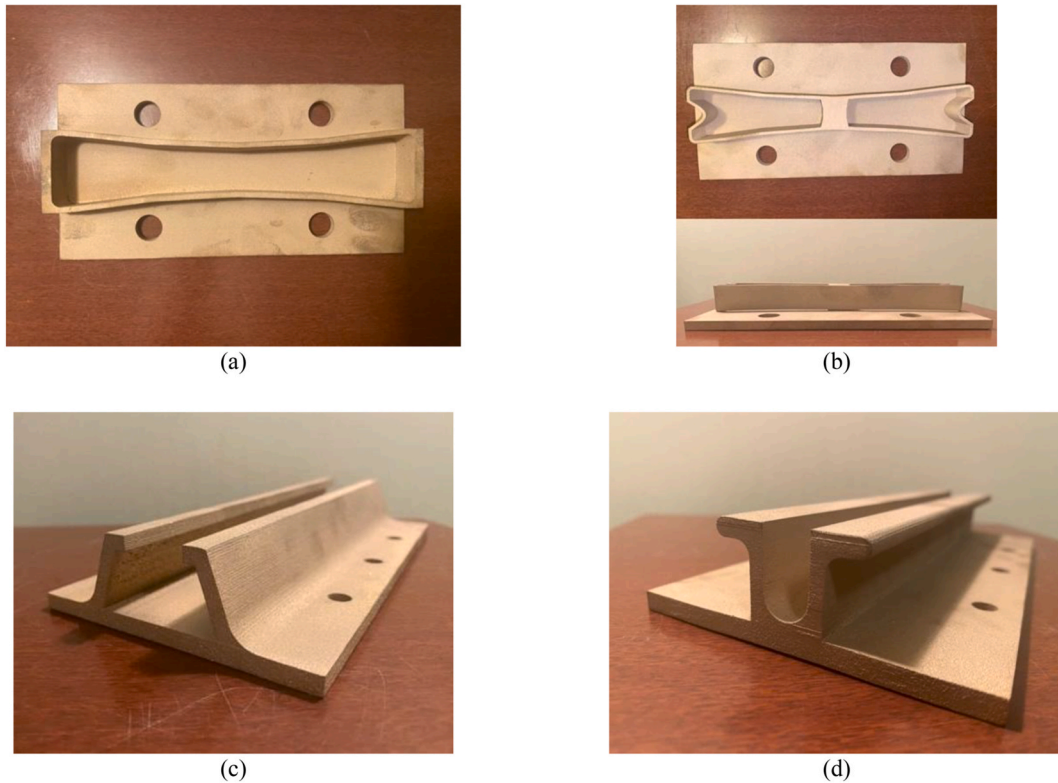


Fig. 10. 3D printed connection specimens: (a) shear female connector; (b) shear male connector; (c) tensile female connector; (d) tensile male connector.

3.2. Coupon test of 3D printed steel material

After the test, tensile coupon tests were undertaken to determine the tensile engineering stress-strain properties of the 3D printed SS420/BR in accordance with EN ISO 6892-1 [41] (Fig. 11) and support future numerical validation. Four coupons were machined from the bottom plates of the tested tensile female connectors (Fig. 12(b)), which experienced insignificant deformation during the testing. All specimens were tested in the direction that parallel to the printing direction under a constant speed of 3 mm/min using an Instron testing machine (Fig. 12(a)), with strain being measured by an extensometer attached to the coupons' surface.

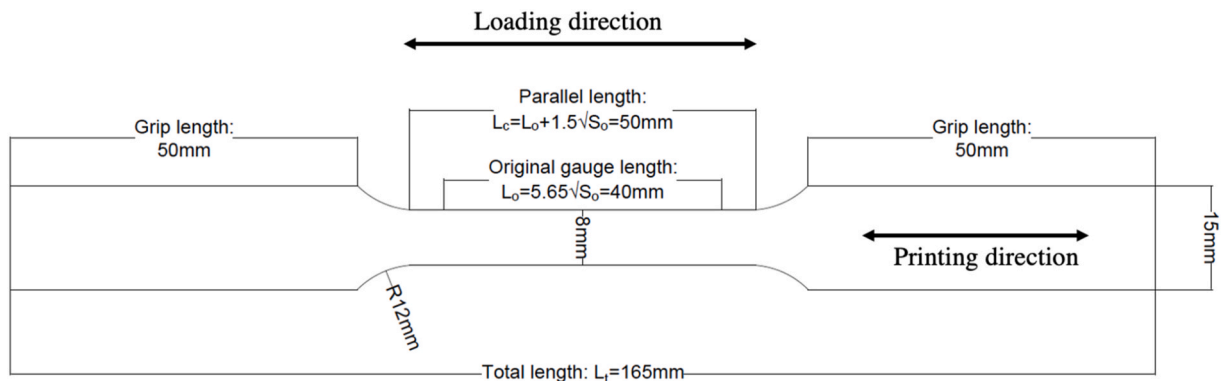


Fig. 11. Dimensions of the coupon specimens according to EN ISO 6892-1 [41].

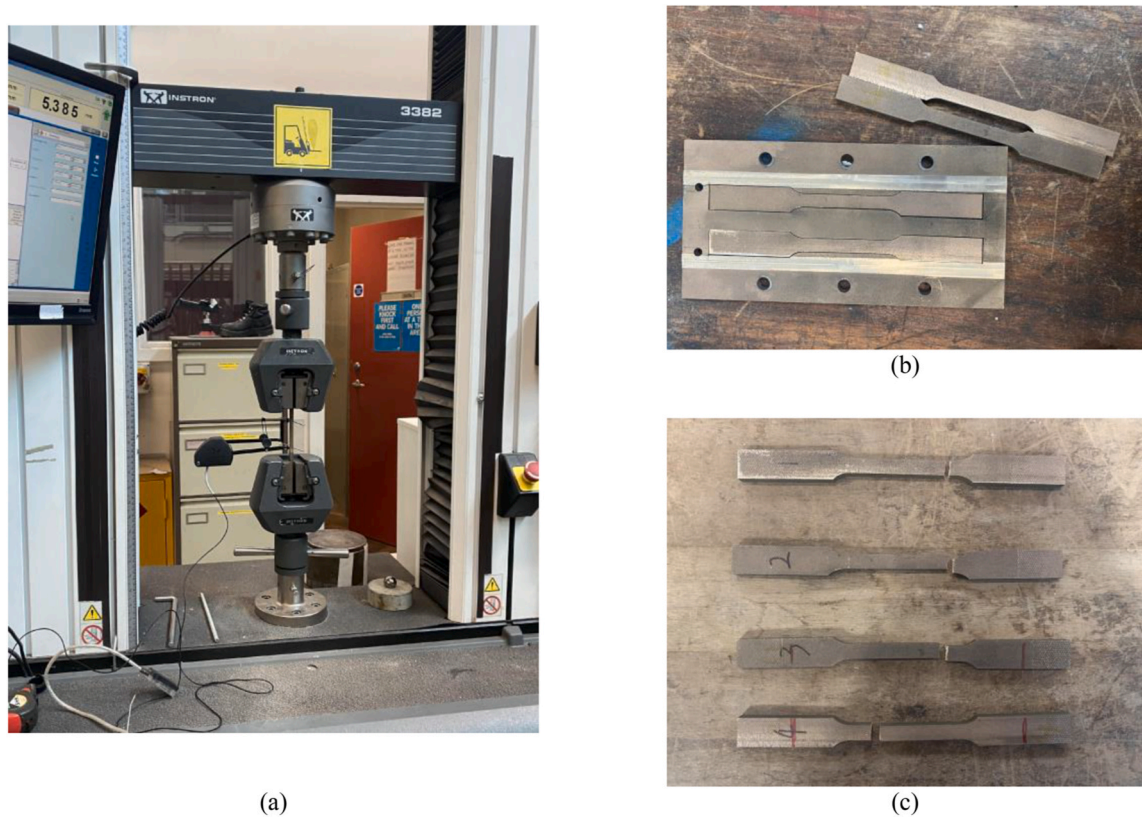


Fig. 12. Coupon test of SS420 (a) set-up for coupon test (b) machined coupons from the bottom plate of the tested tensile female connectors (c) specimens after testing.

The original strain and stress data of the coupon tests were converted into true stress and strain, then the yield strength was calculated accordingly using 0.2% offset method. The generated data were relatively consistent with acceptable variation (Fig. 13), so the averaged properties from 4 coupon tests were adopted in the subsequent numerical study. In comparison with the material properties provided by the manufacturer [40] and the published coupon test data of SS420 [42] with the same printing layer thickness and printing direction, the adopted mean values for simulation have similar Young’s modulus and ultimate strain, while there are

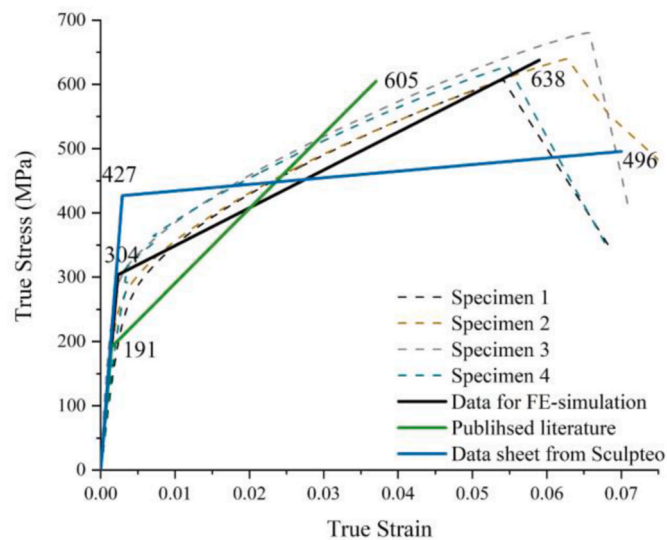


Fig. 13. Experimental data of coupon test and the mean material properties used as input data in simulation.

variations between the yield strength and the ultimate strength. These can attribute to the sensitivity of 3D printing material to the varied printing parameters such as travel speed and sintering temperature from different manufacturers. It should be noted that, 3D printed material has different behaviours in the directions perpendicular to and parallel to the printing direction. However, the variations are only around 2–4% in two printing directions. According to the published experimental data [42], for the same 3D printed material in this research with the same printing layer thickness, the biggest property difference between directions parallel to and perpendicular to the printing direction is 2.1% in the ultimate strength. It can therefore be concluded that, this difference would not affect the results significantly, and the material properties obtained in the printing direction of coupon specimen can well represent the material performance on different directions.

4. Numerical validation model

To validate the numerical models using the experiment output, 3D fully-discretised continuum models of the tensile and shear connections with full details in the unit steel connectors, fasteners and timber were constructed in finite element analysis (FEA) software ABAQUS. Validated modelling methods in publications [43,44] and nominal or tested material properties employed in the validation models, were analysed with ABAQUS/Standard. The dimensions of both connection specimens and the testing set-ups were set to be consistent with the test, as illustrated in Figs. 7 and 8 and 9.

4.1. Modelling methods

4.1.1. Materials

In the models of both tensile and shear connections, the 5-ply CLT panels were modelled using an orthotropic elastoplastic material model with the properties as listed in Table 2. Each layer of the panels was considered separately with the first (20 mm), third (40 mm), and fifth (20 mm) layers being loaded parallel to grain and the second (20 mm) and fourth (20 mm) layers being loaded perpendicular to grain. For all steel fixtures and screws, a Young's modulus of 200 GPa and a poisson's ratio of 0.3 were assumed. Grade-300PLUS steel with a yield strength of 320 MPa and an ultimate strength of 440 MPa was used in all steel fixture devices. The Grade 10.9 carbon steel with a yield strength of 940.3 MPa and an ultimate strength of 940.3 MPa at 0.5% ultimate strain, was adopted for HBSP12120 and LBS7100, which were validated by Tomasi et al. [45]. For the modelling of the 3D printed connectors, a Young's modulus of 130 GPa, a yield strength of 304 MPa, an ultimate strength of 638 MPa and an ultimate strain of 5.9% that extracted from the coupon test were taken. 8-node linear brick with reduced integration (C3D8R) elements were adopted in the mesh throughout the model.

4.1.2. Modelling of shear connection

To better simulate the experiment with sufficient accuracy, the FE model of the shear connection was built according to the experiment set-up (Fig. 14(a)) with full dimensional details of steel fixtures as shown in Fig. 8(a) and connections as shown in Fig. 7(a) on both sides. The movement restrictions in three directions were applied on the steel foundations representing the support from the loading machine, and on the grip bar connecting the entire test set-up to the loading machine. The middle panel with two shear male

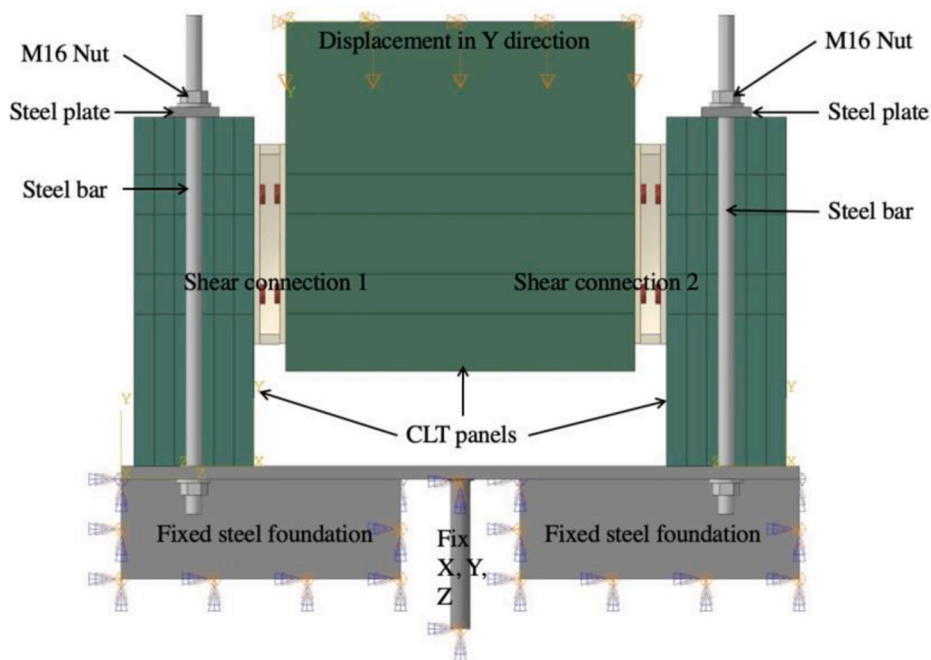


Fig. 14. The outline and boundary conditions of FE model of the shear connection.

connectors attached was loaded in a displacement-controlled manner on top in Y-direction, simulating the load applied in the experiment (see Fig. 14).

In the models of timber connections, the interfaces between timber and steel fasteners are crucial to the overall accuracy of the simulation. When loaded in shear, the screws in timber connections are mainly subjected to compression from the surrounding timber and the steel plate, which is mainly bored by the shank part of screws. Consequently, the screws in interlocking shear connection were modelled as cylindrical elements with a diameter equals to d_s in Table 3. The surface-to-surface discretisation method was adopted for the contact of all interfaces in the model with the “Hard Contact” option in the normal direction, and the “penalty friction formulation” option in the tangential direction, while using a coefficient of friction of 0.4 for all steel-steel contacts [43] and 0.25 for all steel-CLT contacts [46]. Tie constraints were adopted in all interfaces between nuts and threaded bars to simulate the fastening effect, as no relative movements was observed during the test. In the tangential direction of the screws-timber interfaces, a non-linear relation of contact pressure and displacement (Eq. (2)) (Fig. 15) was used in the normal direction along with the “Tabular” option in ABAQUS to simulate the weakening effect of pre-drilling on the timber around screws, considering the chunky screws used in the shear connections.

$$\left(\frac{u_{inter}}{u_0}\right)^{n_u} + \left(\frac{\sigma_0 - \sigma_L}{\sigma_0}\right)^{n_\sigma} = 1 \tag{2}$$

Where n_u and n_σ are the control factors of the function curvature and were taken as 3.9 and 1.1, the contact deformation u_0 was taken as 0.35 mm, all of which were extracted from the test on $\varnothing 12$ dowels conducted by Dorn [47]. σ_0 is the maximum compressive strength of timber that was assumed to be 30 MPa [43]. This formula represents the low timber strength around the surface of screws. Once the deformed screws reach the unaffected area, the strength of timber will be recovered.

4.1.3. Modelling of tensile connection

Similar to the shear connection model, the boundary conditions in the tensile connection model were set according to the experiment set-up. A simplified steel fixture was modelled for applying the movement restrictions as shown in Fig. 16. Displacement-controlled loading in the Y-direction was applied on the steel fixture on the panel with the male connector.

When simulating timber screwed connections loaded in tension, two modelling methods are commonly adopted. The first one is to build the complete model of the screws including full details of the threaded part [48], thus the performance of screws is fully dependent on the geometric characteristics of screws and no assumption of screw properties is needed. The second one is a simplified

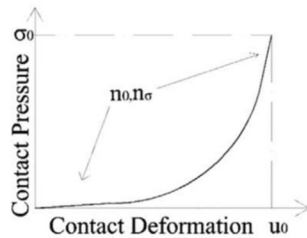


Fig. 15. Function represents the weaken timber around fasteners [43].

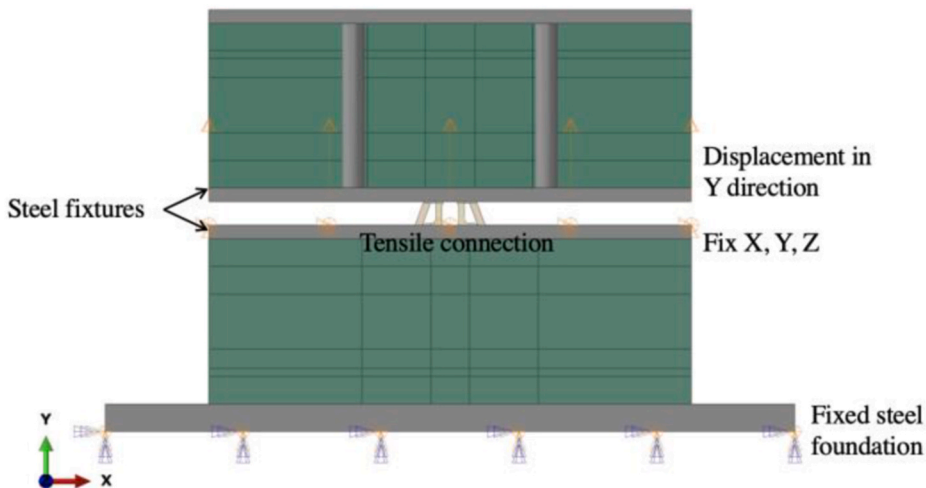


Fig. 16. The outline and boundary conditions of FE model of the tensile connection.

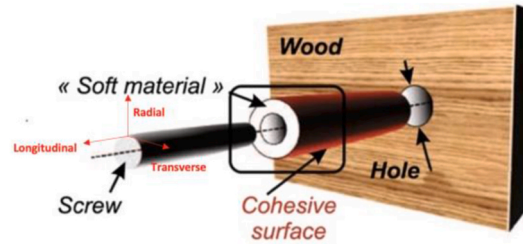


Fig. 17. Simplified FE model for screws in tension [44].

method proposed and validated by Avez et al. [44] and Bedon et al. [49], which introduces a fictitious ‘soft material’ (Fig. 17) to represent the threaded part with the diameter equals to d_1 in Table 3. The ‘soft material’ is assumed to be perfectly elastic and has the same capacity as the wood, except for the radial modulus that is reduced to 50 MPa to eliminate its contribution in the compressive direction, representing the weakening effect of threads on the timber. Wrapped by ‘soft material’ is the ‘core’ that simulates the shank of screws, the dimensional value of which is taken as d_s of LBS7100 (Table 3). Compared to the first method, the second method is computationally more efficient due to the elimination of the small details of the threads and the large contacts areas between the threads and timber, thus it is adopted in this study.

The withdrawal capacity of screws was simulated by a cohesive surface between the internal surface of drilled holes in the timber panel and the external surface of the ‘soft material’ with an assumed rigidity of 40 N/mm^3 in the longitudinal direction and 0 N/mm^3 in the tangential and radial directions (Fig. 17) [44]. The maximum nominal stress (MAXS) approach was applied at the cohesive surface in the ‘damage initiation criterion’ option to simulate the initiation of interaction failure:

$$\max \left\{ \frac{t_n}{t_n^0}, \frac{t_s}{t_s^0}, \frac{t_t}{t_t^0} \right\} = \quad (3)$$

where the t_n^0 , t_s^0 and t_t^0 are the peak allowable stresses in the normal (n), first (s) and second (t) shear direction of the bonding interface, the values of which were taken as 36 MPa, 6.9 MPa and 6.9 MPa, equalling to the compressive and shear strength of timber as listed in Table 2.

After the cohesive resistance is reached, the strength degradation of bonding begins and the brittle post-damage behaviour of the connection under tension interaction was simulated by a ‘linear damage evolution’ law, assuming that the full residual stiffness of the cohesive surface is achieved when 4 mm deformation first attained, so the contact behaviour became elastic-brittle, simulating the brittle failure of dowel-type timber connection under tension. The cohesive interaction was combined with ‘Hard Contact’ in the normal direction and the ‘Penalty Friction Formulation’ with a coefficient of friction of 0.4 in the tangential direction to avoid the penetration of screws into timber at the post-failure stage.

4.1.4. Mesh sensitivity

To study the impact of mesh size on the FE predictions and ensure adequate adoption of mesh size, mesh sensitivity analysis was conducted. The timber panels, fasteners, metal fixtures and the female connectors, which experienced insignificant deformation in the test, were proved to be independent of the mesh size. Therefore, increasingly smaller mesh size was only applied in the interested areas of both connection models (Fig. 18), while the mesh size in other parts of the testing set-up remained consistent. The male connectors of both connections, which are designed to govern connection properties, were first studied with 3 mm mesh size. Then the mesh size was refined to 1.5 mm and 1 mm. It can be observed in Fig. 19(a) that, the changes in mesh size have little impacts on the numerical predictions of shear connector model. In the model of tensile male connector (Fig. 19(b)), the initial stiffness is independent of the mesh size, while yielding strength is slightly sensitive. The 1.5 mm mesh size showed a good compromise between results, accuracy and the calculation efficiency in both models. Hence, it was therefore chosen in the subsequent study.

4.2. Numerical validation

4.2.1. Tensile connection

Fig. 20(a) shows the hysteresis loops for the proposed tensile connections. Different from conventional timber connections, the connection performance in the first cycle of each loading step in cyclic test showed good consistency with the monotonic test, as stiffness and maximum strength in monotonic loading at each step can be reached in cyclic loading without strength degradation, indicating the plastic deformation in the steel male connector does not affect the maximum capacity in the subsequent loading. However, the plastic deformation caused gaps between the two connectors, leading to the sliding of the male connector within the female connector with no reaction force. With the increase of the applied displacement, the bearing walls of the female connector started to open-up and close elastically, along with the upward and downward movement of the male connector. This indicated that the bearing walls also contributed to the connection stiffness under large displacements, which led to the degraded stiffness degradation of each repeated circle, as similar to the pinching effect in the conventional timber connections.

The primary deformation mode in the tensile connection was the bending of the L-shaped elements in the male connector as designed (point 1 in Fig. 20(b)). The female connector and screws on the other hand, remained mostly undeformed (point 2 in Fig. 20

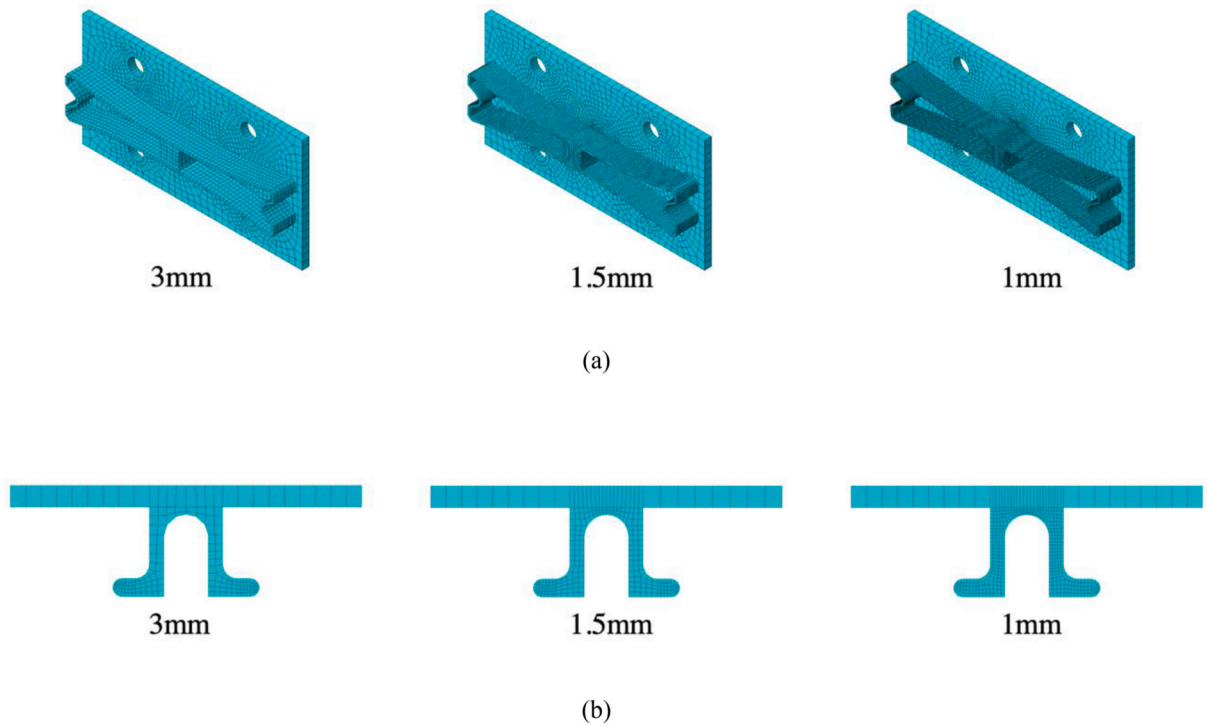


Fig. 18. Mesh size considered in the mesh sensitivity study of (a) shear male connector (b) tensile male connector.

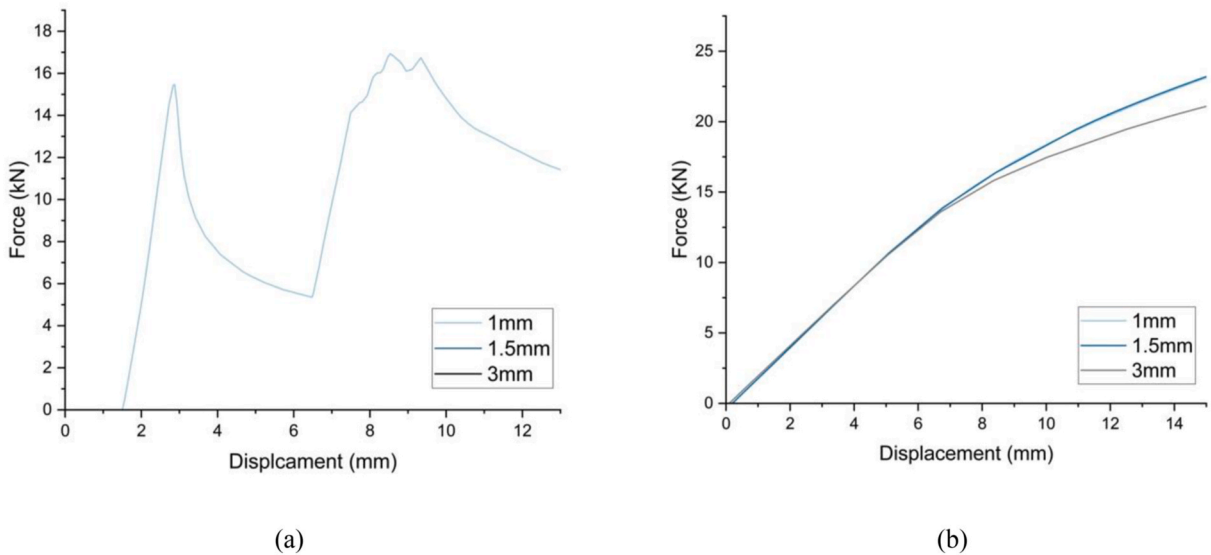


Fig. 19. Fore-displacement response obtained from different mesh size in (a) shear male connector model and (b) tensile male connector model.

(b)), and only very slight open-up in the bearing walls (point 3 in Fig. 20(b)) and slight bending in the bottom plate (point 4 in Fig. 20 (b)) were visible at the end of testing, so the deformed male connector can be easily slide out.

The FE model of the tensile connection showed good agreement with the experimental output, as the maximum strength of each loading cycle, the initial and reduced stiffness can all be well captured. Four deformation modes in the tensile connection, as discussed above, were also well reproduced in terms of shape and dimension, proving the feasibility of the proposed modelling method for interlocking tensile connection. Though slight pulling out can be observed from the screws in the male connector of the model, the continuous force-displacement curve indicated that the screws-timber interfaces still remained elastic, and the ‘linear damage evolution’ in FE model was not activated.

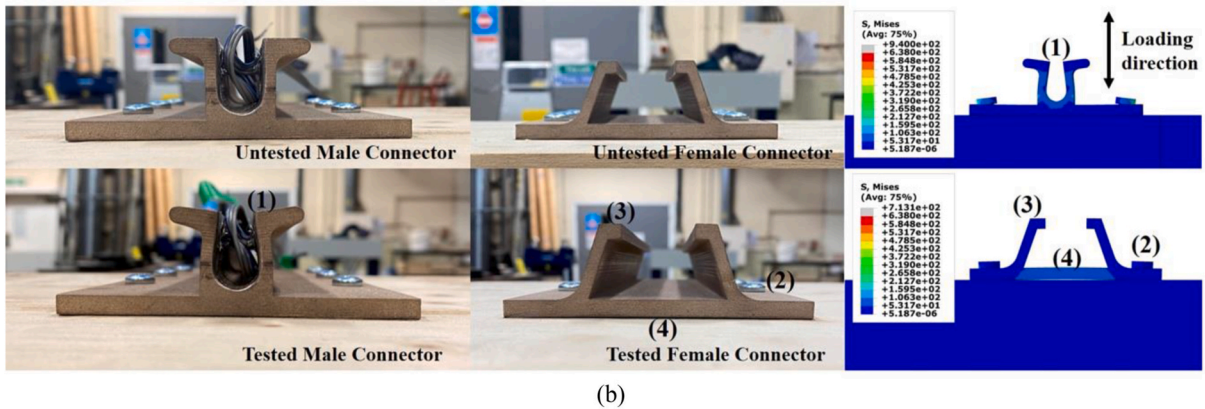
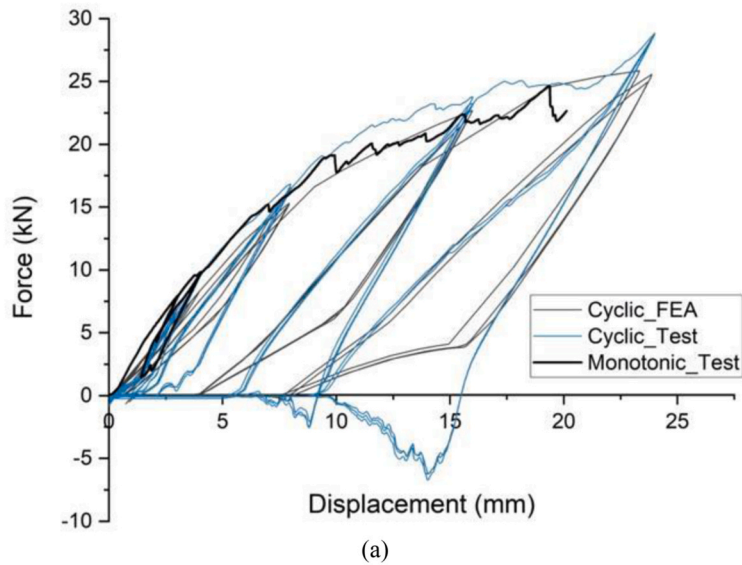


Fig. 20. Comparisons between experimental result and FEA in (a) hysteresis loops and (b) the deformation modes in tensile connection specimens (in mm).

4.2.2. Shear connection

In the cyclic testing of shear connections (Fig. 21(a)), a sudden drop in the force can be observed when first reaching the displacement of 4 mm, which was followed by another one at the displacement of 6.5 mm under the similar forces (around 16 kN). These indicated the buckling happened in the shear connections on both sides (point 1 in Fig. 21(b)), which caused instability in the experimental set-up. After the buckling, the connection strength continued to develop in the deformed steel band and the end sunken (point 2 in Fig. 21(b)), until the breakage happened at the buckling point of one shear connection (Fig. 21(b)), leading to the plumper hysteresis loop at large displacement. Therefore, two major deformation modes can be identified in the tested shear connections after the testing: buckling at the middle of the deformable band and bending at the sunken design at the end of the steel band. As shown in Fig. 21(a), the buckling and plastic deformations in the shear connection specimens caused unsymmetric behaviours in two loading directions, which are unfavourable considering the stability of structures and limit the connection's capacity in dissipating energy. The buckling locations were relatively consistent among all the specimens, while unsymmetric buckling shapes can be observed in some specimens due to manufacturing imperfections and the post-buckling loading on the buckled steel elements.

As buckling was observed in the shear connection, geometrically and materially nonlinear analysis with imperfections (GMNIA) was conducted in the shear connection validation model. The linear Eigen-buckling analysis, which is a common method for predicting the buckling strength and generating 'imperfection' on the model to trigger nonlinear buckling analysis, was first conducted. In the Eigen buckling analysis, a unit pressure was applied at the mid-span to predict the critical load of buckling and the buckling mode shapes of the ideal structure based on the 'Block Lanczos' method. As shown in Fig. 22, the generated four buckling modes in the male connectors on both sides agreed qualitatively with the test results, so they were extracted and imported into the nonlinear analysis as 'imperfection' with a factor of 0.2. As the primary deformation form in the tensile male connector was bending instead of buckling, GMNIA was not considered in the tensile connector model.

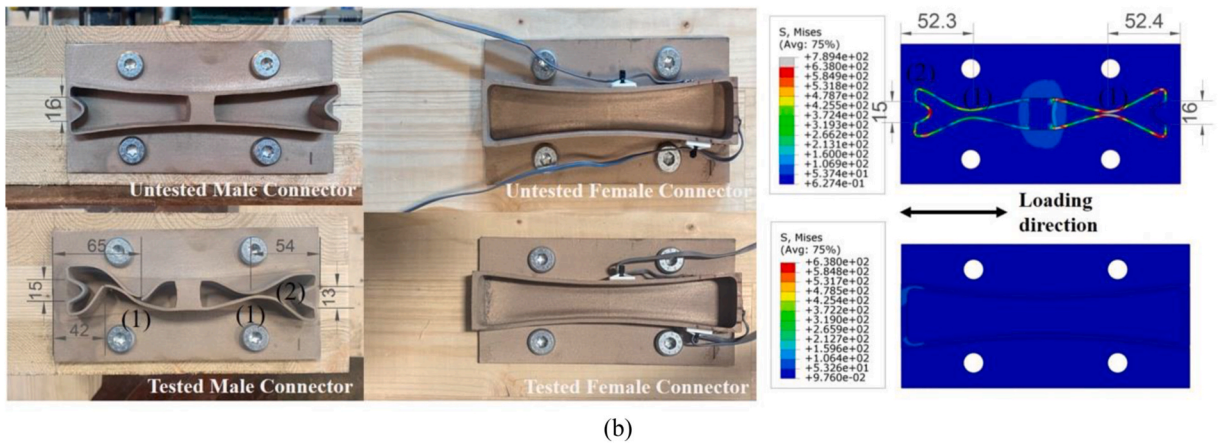
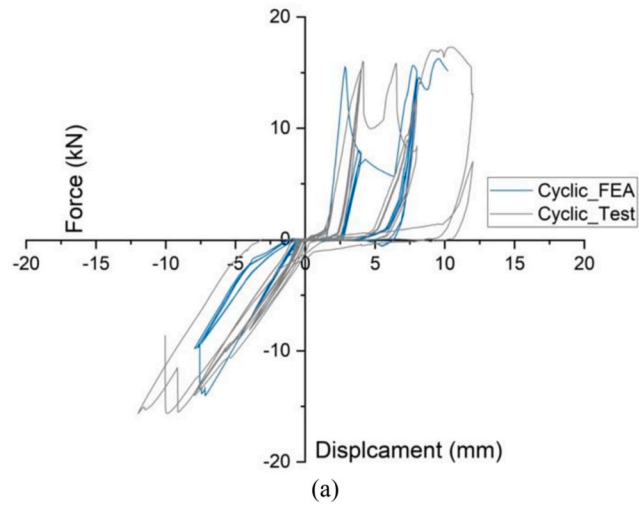


Fig. 21. Comparisons between experimental result and FEA in (a) hysteresis loops and (b) the deformation modes in shear connection specimens at -8mm displacement (in:mm).

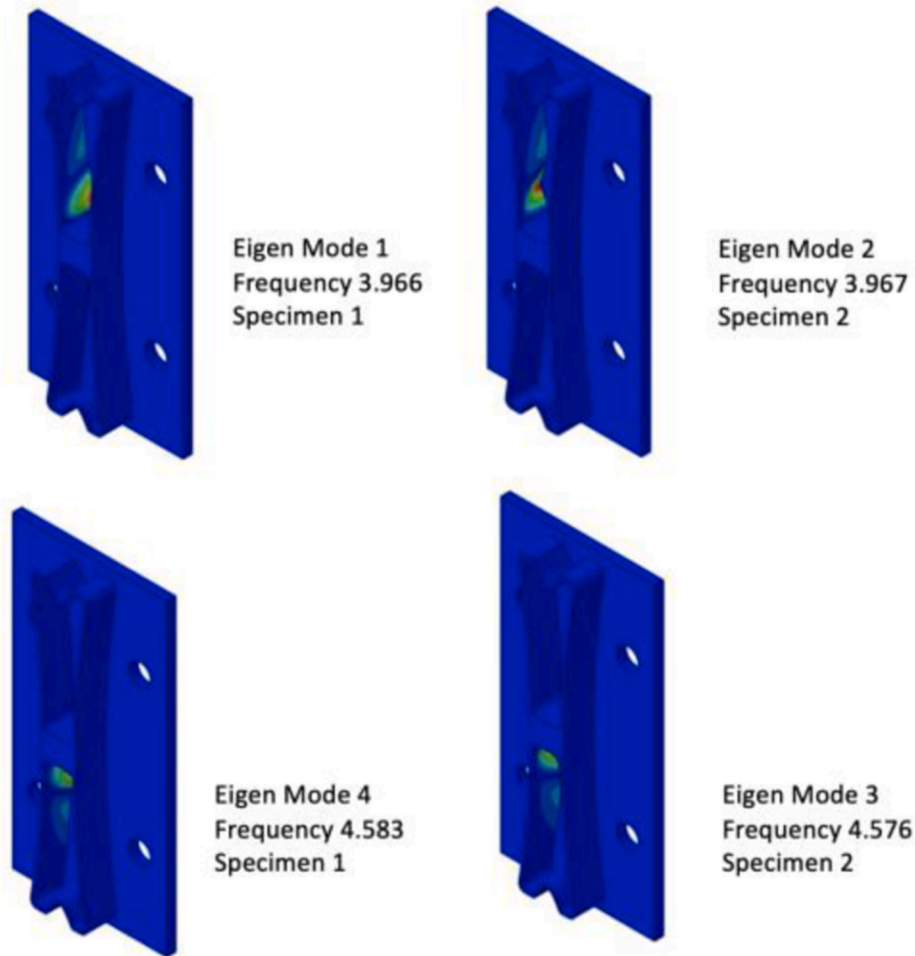


Fig. 22. Four buckling modes extracted by 'Block Lanczos' method.

With the inclusion of 1 mm gap in the shear connection model, sliding in the initial stage of each loading step that corresponding to the experiment can be observed in the numerical output (Fig. 21 (a)). The model with the initial imperfections was able to simulate the negative stiffness of buckling. The buckling shapes on both sides as well as the bending at the end sunken were also well reproduced in terms of locations and dimensions, which proves the adequate accuracy of the validation model.

4.3. Conclusions

The results of the monotonic and cyclic tests on the shear and tensile connections demonstrated that, two connections behaved very differently in terms of mechanical properties and deformation forms. The tensile connection demonstrated lower stiffness but higher maximum strength and better ductility with a ductile failure mode (due to bending), while the shear connection demonstrated higher stiffness but lower maximum strength and ductility with a brittle failure mode (due to buckling). In both connections, there was no sign of pulling out in screws and no visible relative movement between the connectors and timber (Fig. 23) after the attainment of the maximum strength. These indicated that the deformation was successfully managed within the male connectors in both shear and tensile connections, with very small deformation developed in the female connector but without any brittle breakage in timber. This is a clear demonstration of the ability of connections to localise plastic deformation within the male connectors under the control damage approach.

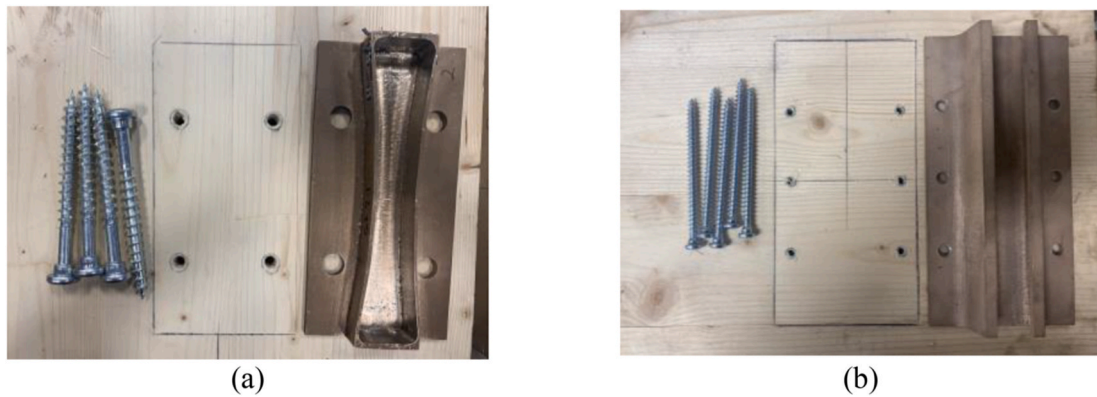


Fig. 23. Removal of screws from (a) shear connections and (b) tensile connection after test.

5. Numerical simulations

To further characterise the translational behaviours of the proposed shear and tensile connections and explore their potential with more common and ductile steel material (S235), a monotonic analysis was performed in the validated models at the primary and the secondary working directions (Fig. 7) of both connections, with material properties of S235 (Young's modulus of 210 GPa, yield strength of 235 MPa and ultimate strength of 360 MPa).

5.1. Translational behaviours of the shear connection

The force-displacement responses of the interlocking shear connection FE model in the primary and secondary directions are reported in Fig. 24. The numerical model can also monitor the deformation developing trends in the shear connections to help better understand the connection behaviours, which was not available in the test due to the concealed design nature of the shear connection. Similar to the tested specimens, the shear connection with S235 first buckled at the cantilevered steel band, resulting in negative stiffness in the FE model. With the continuous loading, the buckled steel band continued to bend and the deformation started to develop in the end sucken on the other side. Corresponding to the experiments, most of the plasticity was observed in the designated deformable band (Fig. 25(a)) in the male connector after a 30 mm displacement in the primary direction, while litter plastic strain was developed in the female connector and fasteners, which also resulted in very small damage on timber panels.

When working in the secondary direction, the interlocking shear connection showed much higher strength and ductility than that in the primary direction, but the process of plastic deformation was mainly managed by the bending of the middle cubic support in the

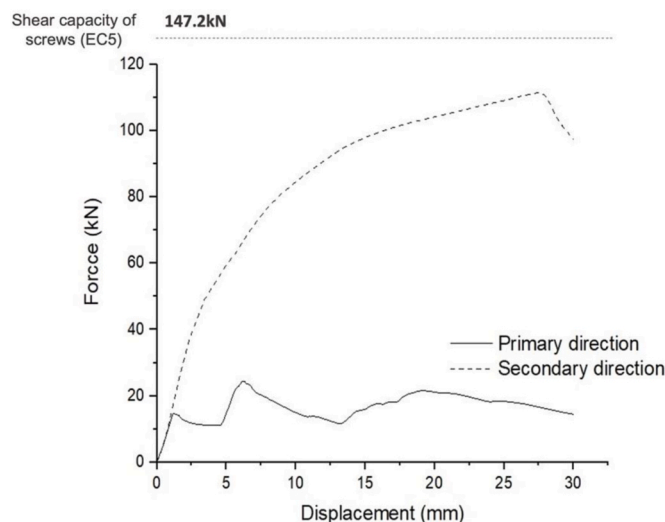


Fig. 24. Force and displacement curve of interlocking shear connection.

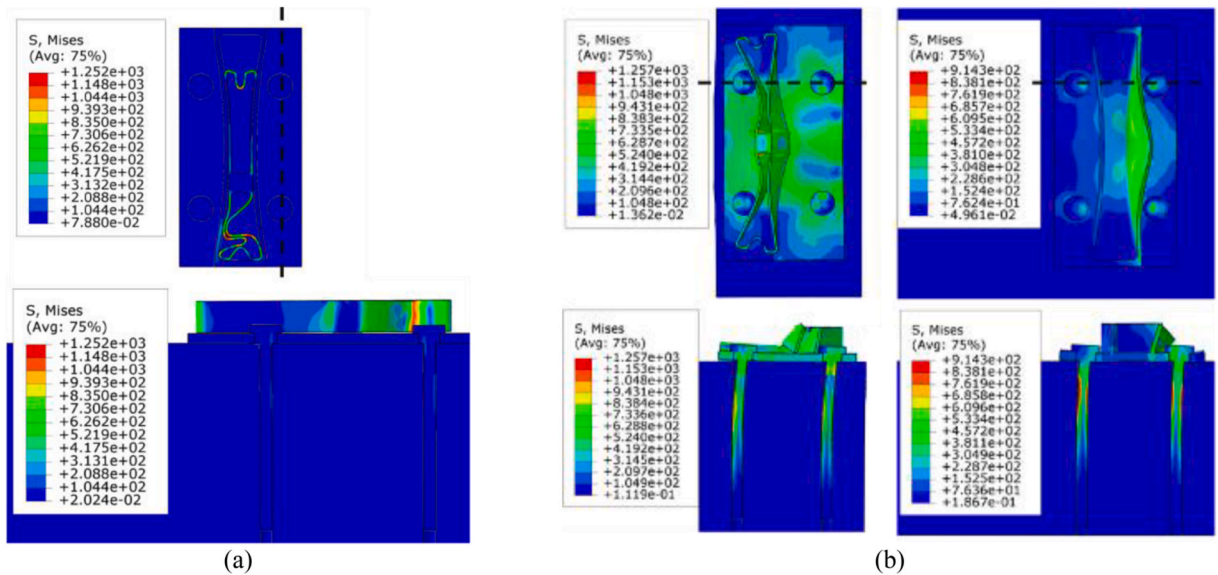


Fig. 25. Stress distribution on shear connections and screws under the displacement of 30 mm in (a) the primary direction and (b) the secondary direction.

male connector and the bending of the wall in the female connector at the loaded side (Fig. 25(b)). The increased plastic strain in the screws proved that the fasteners also contributed to the connection strength when working in the secondary direction.

5.2. Translational behaviours of the tensile connection

As demonstrated in Fig. 26, the behaviour of the interlocking tensile connection with S235 in the primary working direction can be classified into three stages: the elastic stage, the yield plateau stage, and the densification stage. When the loading started, the male

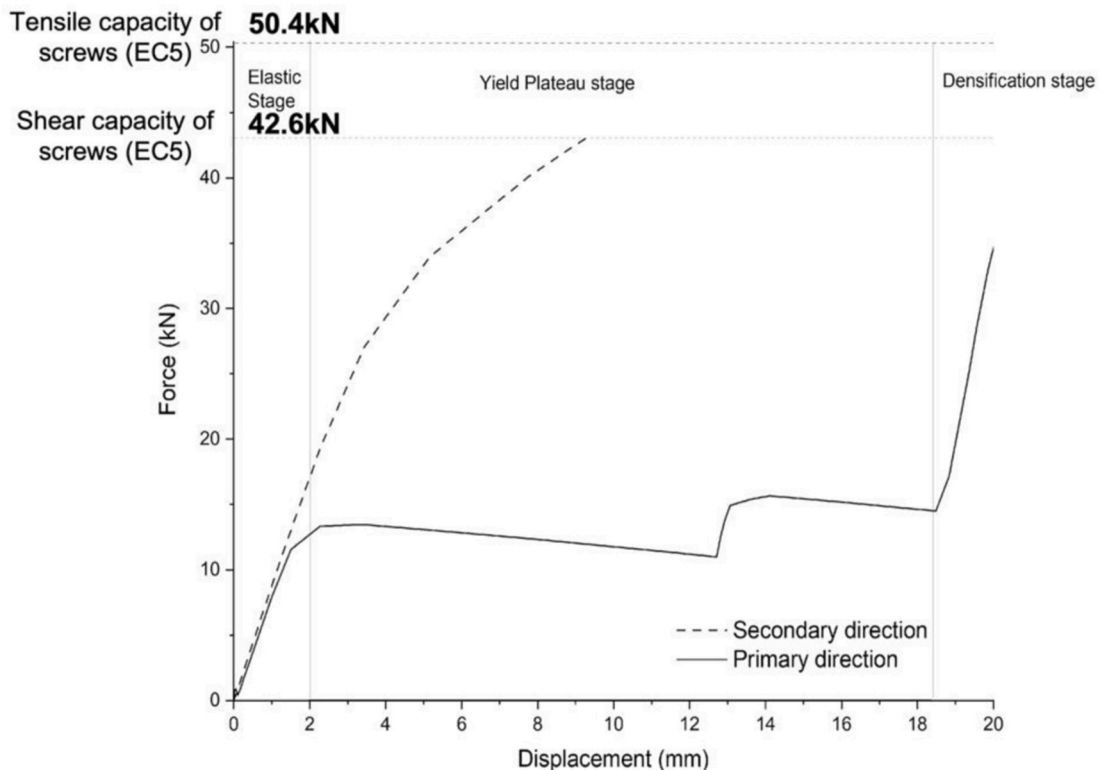


Fig. 26. Force and displacement curve of interlocking tensile connection.

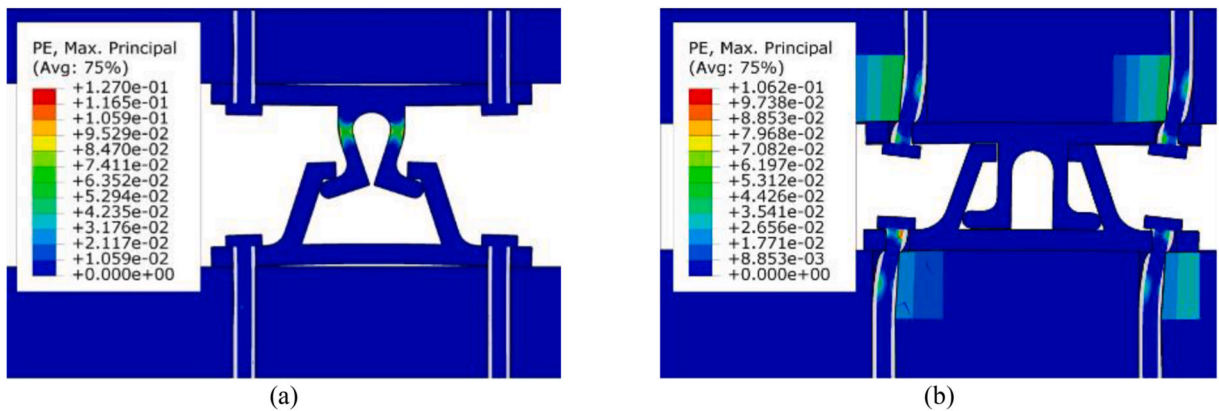


Fig. 27. Von Mises Stress contour in the interlocking tensile connections under the displacement of 15 mm in (a) the primary direction and (b) the secondary direction.

connector started to move upwards within the female connector, and the sloping walls of which compressed the L-shaped elements to bend inwards. With the continuous vertical movement of the male connector, the L-shaped elements yielded and the walls of the female connector started to open up slowly due to the increased moment at the wall base, resulting in slightly decreased reaction force of the connection at the yield plateau stage. When the male connector came into contact with the top of the female connector, it stopped moving and the stiffness of the connection increased significantly, indicating that the behaviour of connection enters the densification stage, in which the connection becomes rigid to prevent further displacement (opening). Thus, the F - δ curve of tensile connection in the primary working direction can be idealised using three parameters: the initial stiffness, the yielding strength and the displacement at the onset of densification. Fig. 27 shows that, at the displacement of 15 mm in the primary working direction, the L-shaped elements in the male connection processed most of the plastic deformation, while little can be observed in other connection components. Though the stress of the screws under tension cannot be reflected directly from the stress contour due to the employment of fictitious elastic 'soft material', no strength reduction can be observed in the force-displacement curve, indicating that brittle failure did not appear in screws at 20 mm slip and the screws were still in the elastic stage.

When loaded in the secondary working direction, the plastic strain contour plot depicts that the interlocking tensile connection developed a similar working mechanism to the conventional steel plate connections, in which the bending of screws and the crushing of timber are the primary deformation modes. The embedment strength of timber and the bending strength of screws therefore became the main contributors of the connection strength, while the interlocking steel connectors were relatively rigid.

6. Discussions and limitations

The FE models of both interlocking shear and tensile connections with S235 demonstrated that the proposed connection designs can provide adequate strength and ductility under translational forces. When working in the primary direction, the male connectors in both connections yielded before reaching the full capacity of the surrounding fasteners, so most of the plastic deformation is managed within the designated areas (male connectors), while the female connectors, fasteners and timber remain mostly intact. This indicates that the dissipating element in the novel interlocking connection shifts from the fasteners like in conventional connections to the steel elements in the new connection. With the specially designed deformable steel elements, this connection system can absorb energy in predictable manners, preventing plastic deformation from developing in fasteners and timber to avoid brittle failure and reducing the risk of significant failure of structures under extraordinary loads such as seismic load. In addition, the initial deformation of the steel male connectors can be monitored and act as an early warning system since they can be relatively easy to access. This also means that only the male connector would fail after a severe event and needs to be repaired or replaced, while the screws connecting the unit and the panel will remain intact, thus the timber fibres will not be affected by the bending of the screws as it is normally the case. It therefore helps to improve the structural integrity and to reduce the time needed for maintenance. When damage happens in the connection units, the damaged module with the male connector can be removed following the installation sequence for the repair or replacement. Due to the short unit length of connection (same to the steel specimen dimensions), rapid and cost-effective supply can be achieved with 3D printing of the male connector. Also, the timber panels can be fully reused since the proposed novel connection system promotes no fastener failure.

In the secondary working direction, the deformation in the connection is less ductile and managed by the composite effect between the fasteners and the steel connector, which is similar to the working mechanism of the conventional steel plate connections and is characterised by its high stiffness but relatively lower ductility than in the primary working direction. When comparing the deformation forms in two working directions, the significantly reduced deformation in screws in the primary direction indicates the successful damage control in connections through the introduction of the proposed connector design.

Different from other novel connections for CLT volumetric structures, the one proposed in this study requires no modifications for fitting, thus is applicable to different flat module specifications. The equipped damage-limiting capacity also makes it superior to the conventional connection in terms of life-safety performance and material reuse after the end-of-life of structures. The proposed

connection system holds the potential of improving the dismantlability in CLT volumetric structures, promoting a more flexible volumetric construction with changeable, demountable and fully reusable structural elements.

Despite the superiorities, the immediate practical application of the proposed connection system may be limited by the existing construction tools. The sliding and stacking of modules require specially-designed lifting and moving machines and scaffolds frames. Also, due to the geometric complexity, the mass production of the proposed connections is difficult to be achieved with the conventional manufacturing methods. However, with the gradually increasing manufacturing scale of 3D printing and the reducing printing cost, the mass production is expected to be achievable with 3D printing in the future.

7. Conclusions

In this paper, a comprehensive review of the recent advancements in the study of connection systems for CLT volumetric structures is first provided. The factors that relate to connection systems and constrain the development of multi-storey CLT volumetric structures have been analysed and summarised. As a result, a novel interlocking connection system is then proposed for addressing the low construction efficiency, inaccessibility of inter-module connections and the insufficient ductility of typical timber connections in VTC. The designed ability of managing deformations within one part of the connection and eliminating damage in timber panels in the primary working direction was proved via experiments and numerical analyses on the 3D printed connection specimens. Numerical models with good accuracy were proposed for both connections using only nominal material properties, owing to the fact that the load-carrying capacity and ductility are correlated to the proposed interlocking metal connectors. Ultimately, the adequate translational strength and ductility of the proposed connections were proved by the validated numerical models.

Future research will include a comprehensive parametric study to identify the critical parameters of the proposed connection systems and their detailed mechanical properties, as well as conduct a direct comparative study between typical connections and the novel connection system via global models of a full-scale CLT volumetric building. The study will be centred to the contribution of the connections to the overall lateral resistance of the structure.

Declaration of competing interest

The authors declare that they have no known competing financial interests or personal relationships that could have appeared to influence the work reported in this paper.

Data availability

No data was used for the research described in the article.

Acknowledgements

The authors and the 3DMBC (<https://3dmbc.com>) group members would like to acknowledge the Royal Academy of Engineering and The Leverhulme Trust funds [LTSRF1819_15_40] as well as The Henry Lester Trust funds for their financial support in 3D printing the connection specimens. The contribution of The George Earle Laboratory staff is also acknowledged for providing technical expertise for the experimental testing. The authors would also like to recognise the support from Rothoblaas and Stora Enso on the testing materials (screws and CLT panels).

References

- [1] T. Duncheva, Fiona F. Bradley, Multifaceted productivity comparison of off-Site timber manufacturing strategies in mainland Europe and the United Kingdom, *Journal of construction engineering and management* 145 (8) (2019), 105244.
- [2] L.F. Carvalho, L.F.C. Jorge, R. Jerónimo, Plug-and-Play multistorey mass timber buildings: Achievements and potentials, *J. Architect. Eng.* 26 (2) (2020).
- [3] M. Stepinac, I. Šušteršič, I. Gavrić, V. Rajčić, Seismic design of timber buildings: highlighted challenges and future trends, *Appl. Sci.* 10 (4) (2020) 1380.
- [4] M. Fragiaco, B. Dujic, I. Sustersic, Elastic and ductile design of multi-storey crosslam massive wooden buildings under seismic actions, *Eng. Struct.* 33 (11) (2011) 3043–3053.
- [5] L. Pozza, R. Scotta, D. Trutalli, M. Pinna, A. Polastri, P. Bertoni, Experimental and numerical analyses of new massive wooden shear-wall systems, *Buildings* 4 (3) (2014) 355–374.
- [6] C. Sandhaas, A. Ceccotti, Earthquake resistance of multi-storey massive timber buildings, in: *forum holzbau* 12, 2012.
- [7] A. Ceccotti, C. Sandhaas, M. Okabe, M. Yasumura, C. Minowa, N. Kawai, SOFIE project - 3D shaking table test on a seven-storey full-scale cross-laminated timber building, *Earthq. Eng. Struct. Dynam.* 42 (13) (2013) 2003–2021.
- [8] I. Gavric, M. Fragiaco, A. Ceccotti, Cyclic behaviour of typical metal connectors for cross-laminated (CLT) structures, *Mater. Struct.* 48 (6) (2015) 1841–1857.
- [9] Z. Li, K.D. Tsavdaridis, L. Gardner, A Review of Optimised Additively Manufactured Steel Connections for Modular Building Systems, in: *Industrializing Additive Manufacturing Proceedings of AMPA2020, International Conference on Additive Manufacturing in Products and Applications (AMPA 2020)*, Zurich, Switzerland, 2020, pp. 357–373.
- [10] K.A. Malo, R.B. Abrahamsen, M.A. Bjertnæs, Some structural design issues of the 14-storey timber framed building “Treet” in Norway, *Eur.J.Wood Wood Prod.* 74 (3) (2016) 407–424.
- [11] Stora Enso, 3–8 storey modular element buildings, Available from: <https://www.storaenso.com/-/media/documents/download-center/documents/product-brochures/wood-products/design-manual-a4-modular-element-buildings20161227finalversion-40en.pdf>.
- [12] C. O’Ceallaigh, A.M. Harte, The elastic and ductile behaviour of CLT wall-floor connections and the influence of fastener length, *Eng. Struct.* 189 (2019) 319–331.
- [13] CEN (European Committee for Standardisation), Eurocode 8 - Design of structures for earthquake resistance - part 1: General rules, seismic actions and rules for buildings, CEN (2004).
- [14] N. Chan, A. Hashemi, P. Zarnani, P. Quenneville, Pinching-free Connector for timber structures, *J. Struct. Eng. (New York, N.Y.)* 147 (5) (2021) 4021036.

- [15] E. Iacovidou, P. Purnell, Mining the physical infrastructure: opportunities, barriers and interventions in promoting structural components reuse, *Sci. Total Environ.* 557–558 (2016) 791–807.
- [16] CEN (European Committee for Standardisation), Eurocode 5 - Design of timber structures - part 1-1: general common rules and rules for buildings, CEN (2014).
- [17] D. Trutalli, L. Marchi, R. Scotta, L. Pozza, Capacity design of traditional and innovative ductile connections for earthquake-resistant CLT structures, *Bull. Earthq. Eng.* 17 (4) (2019) 2115–2136.
- [18] A. Jorissen, M. Fragiaco, General notes on ductility in timber structures, *Eng. Struct.* 33 (11) (2011) 2987–2997.
- [19] M. Izzi, D. Casagrande, S. Bezzi, D. Pasca, M. Follesa, R. Tomasi, Seismic behaviour of Cross-Laminated Timber structures: a state-of-the-art review, *Eng. Struct.* 170 (2018) 42–52.
- [20] M. Izzi, A. Polastri, M. Fragiaco, Modelling the mechanical behaviour of typical wall-to-floor connection systems for cross-laminated timber structures, *Eng. Struct.* 162 (2018) 270–282.
- [21] P. Sharafi, M. Mortazavi, B. Samali, H. Ronagh, Interlocking system for enhancing the integrity of multi-storey modular buildings, *Autom. Construct.* 85 (2018) 263–272.
- [22] J. Di Pasquale, F. Innella, Y. Bai, Structural concept and solution for hybrid modular buildings with removable modules, *J. Architect. Eng.* 26 (3) (2020), 4020032.
- [23] R. Gijzen, Modular Cross-Laminated Timber Buildings, in *the Faculty of Civil Engineering And Geosciences*, Delft University of Technology, 2017.
- [24] C. Zhang, G. Lee, F. Lam, Connections for Stackable Heavy Timber Modules in Midrise to Tall Wood Buildings, *Timber Engineering and Applied Mechanics (TEAM) Laboratory*, 2019.
- [25] Rothoblaas, LOCK T: concealed hook timber-to-timber connector, Available from: <https://www.rothoblaas.com/products/fastening/brackets-and-plates/concealed-connections/lock-t>.
- [26] Z. Li, X. Wang, M. He, Z. Shu, Y. Huang, A. Wu, Mechanical performance of pre-fabricated metal dovetail connections for Cross-Laminated Timber (CLT) structures, *Construct. Build. Mater.* 303 (2021) 124468.
- [27] D. Fitzgerald, T.H. Miller, A. Sinha, J.A. Nairn, Cross-laminated timber rocking walls with slip-friction connections, *Eng. Struct.* 220 (2020), 110973.
- [28] D. Fitzgerald, A. Sinha, T.H. Miller, J.A. Nairn, Axial slip-friction connections for cross-laminated timber, *Eng. Struct.* 228 (2021), 111478.
- [29] A. Hashemi, P. Zarnani, R. Masoudnia, P. Quenneville, Experimental testing of rocking cross-laminated timber walls with resilient slip friction joints, *J. Struct. Eng.* 144 (2018), 4017180.
- [30] J. Schneider, T. Tannert, S. Tesfamariam, S.F. Stiemer, Experimental assessment of a novel steel tube connector in cross-laminated timber, *Eng. Struct.* 177 (2018) 283–290.
- [31] S. Dires, T. Tannert, Performance of coupled CLT shear walls with internal perforated steel plates as vertical joints and hold-downs, *Construct. Build. Mater.* 346 (2022), 128389.
- [32] A. Kramer, A.R. Barbosa, A. Sinha, Performance of steel energy dissipators connected to cross-laminated timber wall panels subjected to tension and cyclic loading, *J. Struct. Eng.* 142 (4) (2016), 4015013.
- [33] F. Sarti, A. Palermo, S. Pampanin, Fuse-type external replaceable dissipators: experimental Program and numerical modelling, *J. Struct. Eng. (New York, N.Y.)* 142 (12) (2016), 4016134.
- [34] A. Hashemi, P. Zarnani, R. Masoudnia, P. Quenneville, Seismic resistant rocking coupled walls with innovative Resilient Slip Friction (RSF) joints, *J. Constr. Steel Res.* 129 (2017) 215–226.
- [35] A. Baird, T.J. Smith, A. Palermo, S. Pampanin, Experimental and numerical study of U-shape flexural plate (UFP) dissipators, in: 2014 NZSEE Conference, New Zealand, Auckland, 2014.
- [36] B.H. Xu, M. Taazount, A. Bouchaïr, P. Racher, Numerical 3D finite element modelling and experimental tests for dowel-type timber joints, *Construct. Build. Mater.* 23 (9) (2009) 3043–3052.
- [37] British Standards Institution, BS EN 12512:2001 Timber Structures - Test Methods. Cyclic Testing of Joints Made with Mechanical Fasteners, British Standards Institution (2001).
- [38] British Standards Institution, BS EN 1380:2009 Timber Structures - Test Methods. Load Bearing Nails, Screws, Dowels and Bolts, British Standards Institution (2009).
- [39] C. Sandhaas, Mechanical Behaviour of Timber Joints with Slotted-In Steel Plates, Delft University of Technology, *Netherlands*, 2012.
- [40] Sculpteo, Steel/Bronze 420SS/BR material guide, Available from: <https://www.sculpteo.com/en/materials/binder-jetting-material/binder-jetting-stainless-steel-material/>.
- [41] British Standards Institution, BS EN ISO 6892-1:2019 Metallic Materials. Tensile Testing. Method of Test at Room Temperature, British Standards Institute, 2016.
- [42] M. Doyle, K. Agarwal, W. Sealy, K. Schull, Effect of layer thickness and orientation on mechanical behavior of binder jet stainless steel 420 + Bronze parts, *Procedia Manuf.* 1 (2015) 251–262.
- [43] A. Hassanieh, H.R. Valipour, M.A. Bradford, Sandhaas, C. Modelling of steel-timber composite connections: validation of finite element model and parametric study, *Eng. Struct.* 138 (2017) 35–49.
- [44] C. Avez, T. Descamps, E. Serrano, L. Léoskool, Finite element modelling of inclined screwed timber to timber connections with a large gap between the elements, *Eur. J. Wood Wood Prod.* 74 (3) (2016) 467–471.
- [45] R. Tomasi, A. Crosatti, M. Piazza, Theoretical and experimental analysis of timber-to-timber joints connected with inclined screws, *Construct. Build. Mater.* 24 (9) (2010) 1560–1571.
- [46] X. Liu, M.A. Bradford, M.S.S. Lee, Behavior of high-strength friction-grip bolted shear connectors in sustainable composite beams, *J. Struct. Eng.* 141 (6) (2015), 4014149.
- [47] M. Dorn, Investigations on the Serviceability Limit State of Dowel-type Timber Connections, Vienna University of Technology, 2012. PhD dissertation.
- [48] S. Nassiri, Z. Chen, A. Lamanna, W. Cofer, Numerical simulation of failure mechanism in screw anchors under static tension, *Adv. Struct. Eng.* 23 (16) (2020) 3385–3400.
- [49] C. Bedon, M. Fragiaco, Numerical analysis of timber-to-timber joints and composite beams with inclined self-tapping screws, *Compos. Struct.* 207 (2019) 13–28.